A BENCH SCALE COMPARISON OF BATCH AND CONTINUOUS SETTLING

A BENCH SCALE COMPARISON OF BATCH AND CONTINUOUS SETTLING

By

HOWARD R. HEFFLER, B.Sc. ENG.

A Thesis

Submitted to the Faculty of Graduate Studies

in Partial Fulfilment of the Requirements

for the Degree

Master of Engineering

McMaster University

(1971)

MASTER OF ENGINEERING (1971) McMASTER UNIVERSITY
(Chemical Engineering) Hamilton, Ontario

TITLE: A Bench Scale Comparison of Batch and Continuous Settling

AUTHOR: Howard Russell Heffler, B.Sc. Eng. (University of New Brunswick)

SUPERVISOR: Dr. K.L. Murphy

NUMBER OF PAGES: vi, 67

SCOPE AND CONTENTS:

A bench scale continuous settling unit was constructed and its operation compared to results of batch settling tests. The particulate solids used were polystyrene spheres with a mean diameter of 285 microns. The concentration profile within the slurry in both the batch and the continuous studies was observed using a light extinction technique.

The results show that for the material used in this study, the solids flux limitation of the continuous settler could not be exceeded: the limiting condition in the operation was always the clarification capacity or upward velocity. The batch flux plot shows that this will be the case for any material which exhibits a flux plot that is essentially a single concave curve downwards.

ACKNOWLEDGEMENTS

The author wishes to express his indebtedness and gratitude to Dr. K.L. Murphy for his assistance and guidance throughout the course of this work.

Financial assistance for this work was provided by the Department of Chemical Engineering.

The writer also wishes to thank Miss Dorothy Seeto who typed this report. The responsibility for any errors of omission or commission, however, rests with the author.

Howard R. Heffler

TABLE OF CONTENTS

Chapter			Page
1		INTRODUCTION	1
2		THEORY AND LITERATURE REVIEW	3
	2.1	Batch Settling	3
	2.2	Continuous Settling	14
	2.3	Experimental Studies	24
3		EXPERIMENTAL APPARATUS AND PROCEDURE	28
	3.1	Batch Studies	28
		3.1a Apparatus	28
		3.1b Description of Digital Data Logging System	31
		3.1c Experimental Procedure	33
	3.2	Continuous Settler	35
		3.2a Apparatus	35
		3.2b Operation of the Continuous Settler	37
	3.3	Description of Particulate Solids Used	42
4		EXPERIMENTAL RESULTS AND DISCUSSION	46
	4.1	Batch Studies	46
	4.2	Results from Continuous Settler Studies	54
5		SUMMARY AND CONCLUSIONS	62

REFERENCES
APPENDICES
A - Nomenclature
B - Data
C - Computer Programs
D - Additional References

LIST OF ILLUSTRATIONS

Figure		Page
2.1	BATCH SEDIMENTATION	4
2.2	BATCH SETTLING RATE CURVE	6
2.3	TYPICAL SETTLING CURVES	6
2.4	BATCH CURVE SHOWING CONCENTRATION ZONES	9
2.5	BATCH FLUX PLOT	9
2.6	CONTINUOUS SETTLING UNIT	15
2.7	TALMAGE AND FITCH CONSTRUCTION	19
2.8	BATCH FLUX PLOT CONSTRUCTION	19
2.9	CONTINUOUS FLUX PLOT CONSTRUCTION	22
3.1	DRAWING OF BATCH SETTLING COLUMN	30
3.2	BATCH SETTLING EXPERIMENTAL SYSTEM	32
3.3	DRAWING OF CONTINUOUS APPARATUS	38
3.4	CONTINUOUS SETTLING EXPERIMENTAL SYSTEM	39
3.5	EXPERIMENTAL APPARATUS	40
3.6	CUMULATIVE SIZE DISTRIBUTION OF PARTICLES	43
3.7	PARTICULATE SOLIDS USED IN STUDY	44
4.1	LIGHT TRANSMITTANCE VS. INITIAL SOLIDS FRACTION	48
4.2	OBSERVED BATCH SETTLING CURVES	50
4.3	SETTLING VELOCITY VS. PARTICLE CONCENTRATION	51
4.4	COMPARISON WITH HAPPEL AND BRENNER EQUATION	53
4.5	OBSERVED BATCH FLUX PLOT	55
4.6	BATCH FLUX BY HAPPEL AND BRENNER RELATION	56

LIST OF ILLUSTRATIONS (Contd.)

Figure		Page
4.7	LIGHT TRANSMITTANCE VS. FEED CONCENTRATION	58
4.8	FLUX PLOT CONSTRUCTION	60
4.9	COMPARISON OF BATCH AND CONTINUOUS SETTLING VELOCITIES	62

CHAPTER 1

INTRODUCTION

The design of continuous, gravity settlers for the separation of particulate solids from a slurry is often based on the analysis of batch settling rates. This is a practical approach since, experimentally, batch settling data is relatively easy to obtain. An understanding of the physical phenomena of both batch and continuous settling should allow development of the mathematical technique for design. Such a mathematical technique is available, although it is based on a somewhat idealized description of the settling phenomenon. There is a large amount of literature on the description and analysis of the batch settling mechanism but very little information is available on the operation of continuous settlers which verifies the success of the design procedure. This limited amount of data does, in fact, indicate that the results of this design procedure are not entirely satisfactory.

Several techniques are available for the design of continuous settlers which, although slightly different in detail, are all based on the mathematical analysis of batch settling given by Kynch (1952) and all ideally lead to the same result. Since the Kynch analysis of batch settling is mathematically rigorous, its validity must rest on the underlying assumptions. The fact that the current design procedure is not entirely successful may be attributed to:

(1) the analysis is based on an over-simplified model of settling, or,

(2) full-size settling basins do not follow the idealized theoretical description (e.g. improper hydraulic flow patterns or imperfect solids removal in the underflow may occur).

The object of this study was to construct a bench scale continuous settler conforming as closely as possible to the "idealized" description. In this way the performance of an "idealized" continuous settling unit was evaluated and compared to the predictions from batch data obtained in a geometrically similar system.

CHAPTER 2

THEORY AND LITERATURE REVIEW

Continuous gravity sedimentation offers a very attractive method of separating particulate solids from a liquid slurry. The desired product might be the clarified overflow; clarification, or the concentrated underflow; thickening, or both. In either case design of the unit is based upon the interpretation of batch settling experiments.

2.1 Batch Settling

Historically the first description of batch settling was given by Coe and Clevenger (1916). In spite of the vast amount of work since that time, this original description is still the basis of sedimentation theory.

Initially the slurry is uniformly distributed at its initial concentration in the test cylinder. This is portrayed in Figure 2.1a (zone B). As sedimentation proceeds the slurry settles at a constant rate, dependent on the initial concentration and the nature of the material, establishing a zone (A) of clear liquid and a zone (D) of settled particles at the ultimate concentration (Figure 2.1b). Between "B" and "D" is a zone (C) with concentration varying from the initial concentration at the top to the ultimate concentration at zone D. The volume of zones C and D increases as particles settle into these regions, while concurrently zone A increases at the expense of "B". The liquid-slurry interface (A - B) continues to settle at a constant rate until "B" disappears. After this "critical point" the settling rate constantly decreases as the material settles at a slower

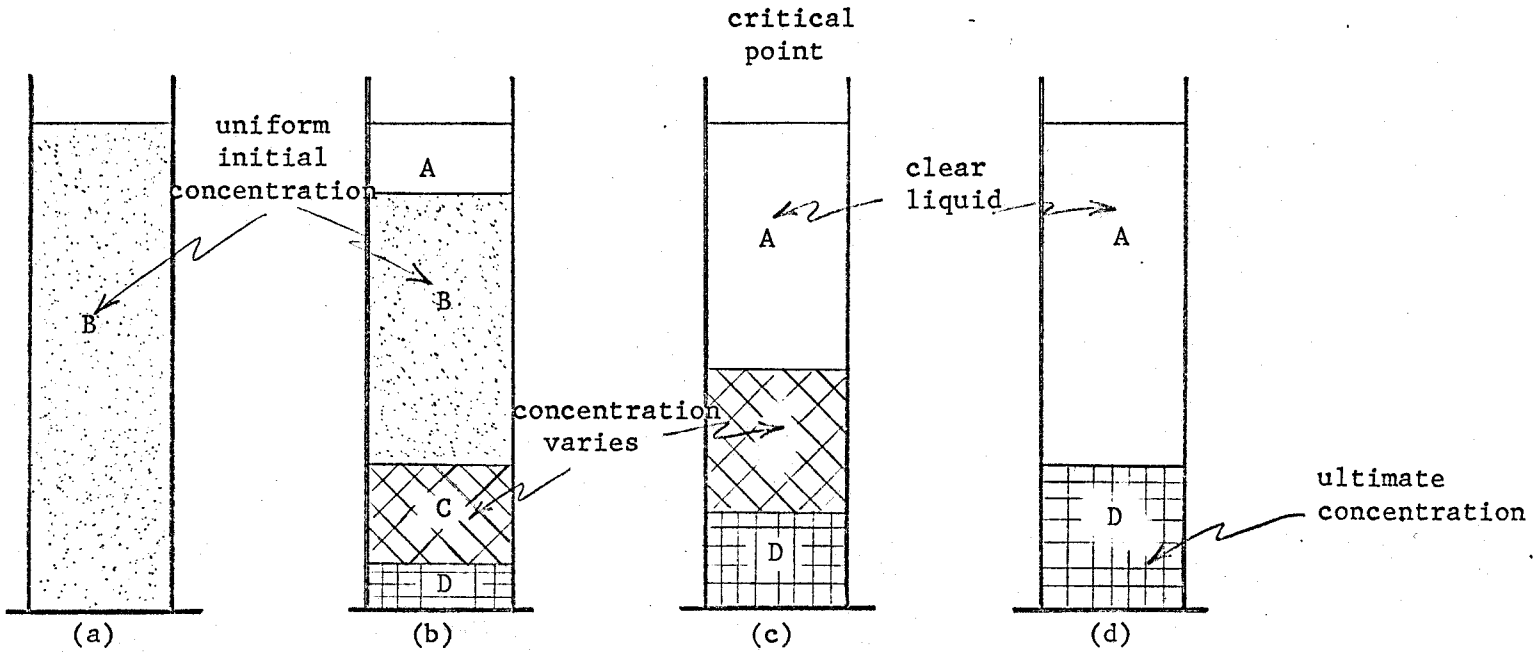

Figure 2.1

Batch Sedimentation

rate until all particles are supported by the bottom (Figure 2.1d). Figure 2.2 shows the height of the liquid-slurry interface plotted as a function of time for this description. The slope of the curve is constant to the critical point and then decreases to zero when the slurry is fully compacted.

With other materials the shape of this curve might show different characteristics. Figure 2.3, curve A, shows the case when the settling rate increases with time as the material flocculates forming faster settling clusters of particles. Curve B shows the case for dilute concentrations of non-interacting (discrete) particles which may settle at a constant rate to the ultimate concentration. The decreasing rate portion of this curve will be very short. Some material, curve C, may settle very slowly at first, presumably until floc formation, and then more quickly until it reaches the start of the decreasing rate phase. This "compression phase" might be very long and exhibit very low settling rates. With this type of material it may be extremely difficult to identify the "initial rate".

The mathematical analysis of batch settling was given by Kynch (1952). This development was based on a single main assumption: that the settling rate is a function only of the local solids concentration. In the analysis it was further assumed that the wall effects were negligible and all particles were identical in their hydraulic characteristics. It was also assumed that the concentration was uniform across the constant, cross-sectional area at each position in the vessel.

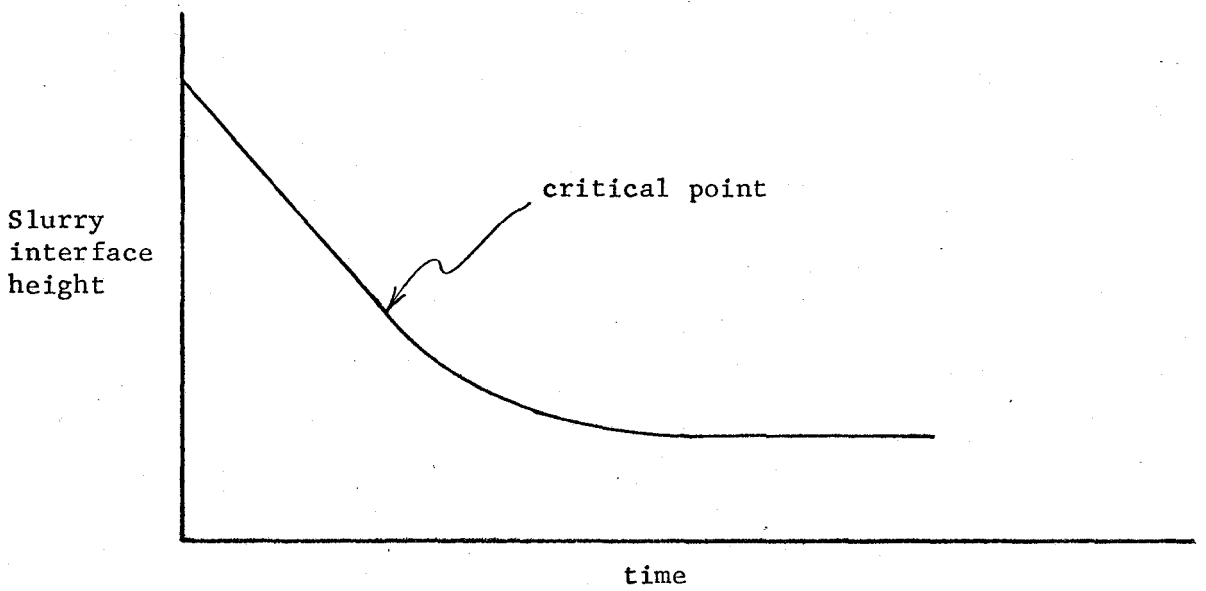

Figure 2.2

Batch Settling Rate Curve

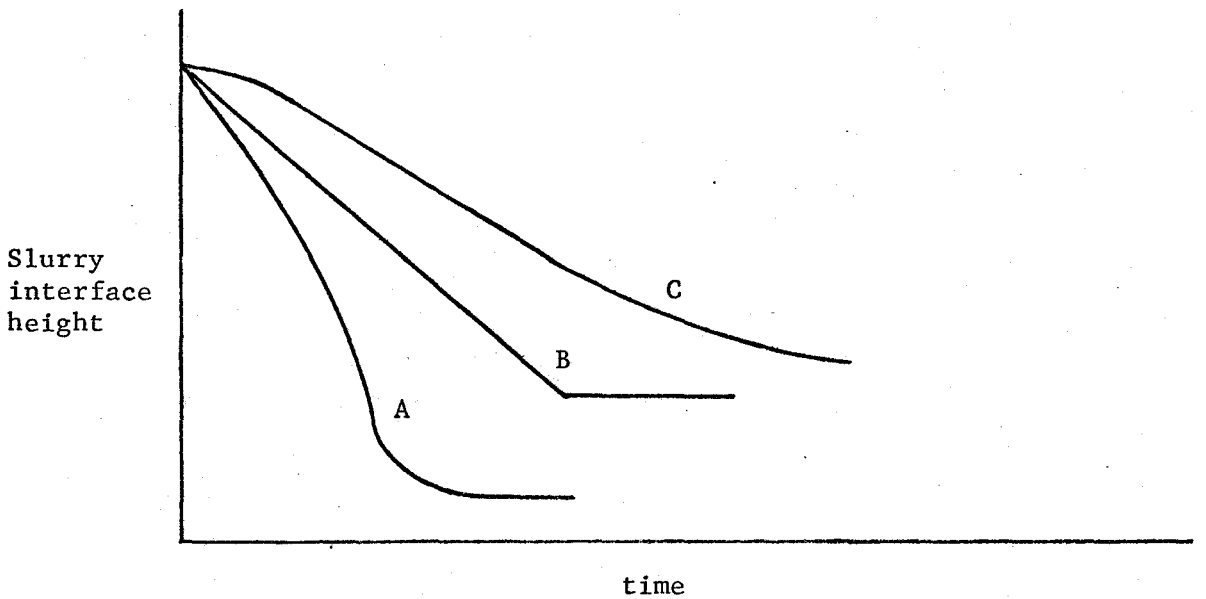

Figure 2.3

Typical Settling Curves

Employing the concept of solids flux:

$$G = Cv \qquad \ldots (1),$$

where: G is the solids flux per unit area,

C is the solids concentration, and

v is the velocity at that concentration.

Consider a horizontal section of thickness Δz across a cylinder of constant cross-sectional area, A, located at position z above the bottom of the column. A solids material balance on the element gives the continuity equation:

Flux in - Flux out = Accumulation

$$\left[G\big|_{z+\Delta z} - G\big|_{z}\right] A\Delta t = \left[C\big|_{t+\Delta t} - C\big|_{t}\right] A\Delta z,$$

or; taking limits,

$$\frac{\partial G}{\partial z} = \frac{\partial C}{\partial t} \qquad \ldots (2).$$

If on a graph of z vs. t a curve of constant concentration is drawn, two points on this curve are (z,t) and (z+dz, t+dt). Then;

$$C(z,t) = C(z+dz,\ t+dt)$$

or,

$$\frac{\partial C}{\partial z}\,dz + \frac{\partial C}{\partial t}\,dt = 0 \qquad \ldots (3).$$

From equation (1),

$$\frac{\partial G}{\partial z} = V(c)\,\frac{\partial C}{\partial z} \qquad \ldots (4),$$

and equating this with equation (2),

$$\frac{\partial C}{\partial t} = V(c)\,\frac{\partial C}{\partial z} \qquad \ldots (5).$$

Inserting equation (5) into (3) gives,

$$\frac{dz}{dt} = -V(c) \qquad \ldots (6),$$

which is a constant since it results from two points on an isoconcentration line.

Note also that by equation (4),

$$V(c) = \frac{dG}{dC} \qquad \ldots (7).$$

If the existence of a small, but finite, change in concentration is allowed at some level in the slurry the solids material balance must be re-written. If this concentration change is to be maintained the rate of solids entering the layer must equal the rate leaving. Since the particle velocity is determined only by local concentration, the only way this concentration discontinuity can be maintained is for it to move upwards through the slurry. Denoting the solids above and below this layer by the subscripts 1 and 2 respectively,

$$C_1(v_1 + u) = C_2(v_2 + u),$$

where, u is the upward velocity of the concentration discontinuity, or,

$$u = \frac{G_1 - G_2}{C_2 - C_1} \qquad \ldots (8).$$

If this discontinuity is infinitesimal,

$$u = -\frac{dG}{dC} \qquad \ldots (9).$$

Comparing equations (7) and (9), it can be seen that V(c) is the rate at which a layer of constant concentration is propagated upward from the bottom of the cylinder to the slurry interface. It is also noted that V(c) is constant for each value of concentration (equation (6)).

Kynch illustrated this concept on a plot of slurry interface position vs. time, Figure 2.4. Between points A and B the slurry settled at a constant rate and in the region defined by triangle AOB the slurry was at its initial concentration. At point B the first concentration change

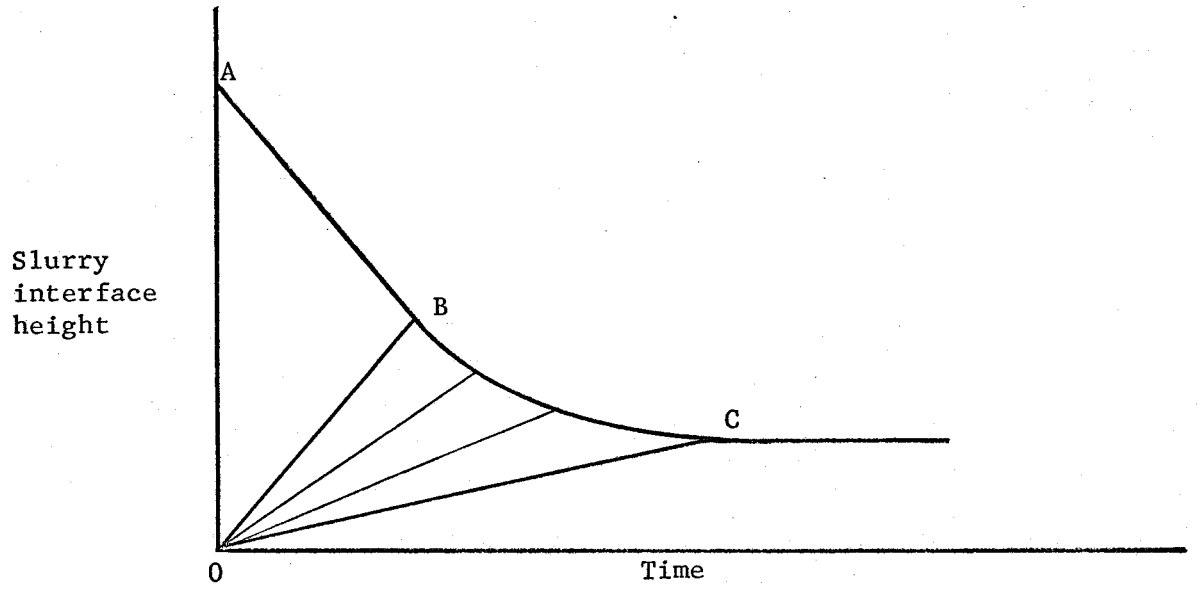

Figure 2.4

Batch Settling Curve Showing Concentration Zones

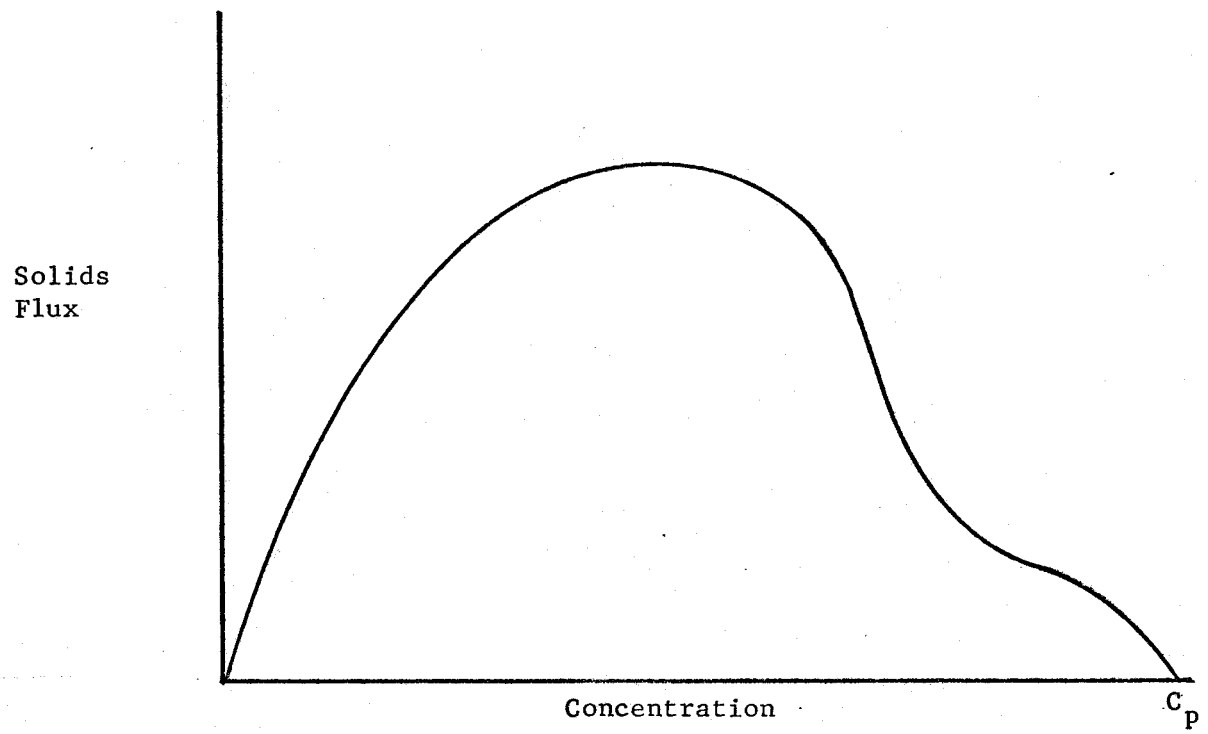

Figure 2.5

Batch Flux Plot

reached the interface and the settling rate began to decrease. As each further concentration change reached the surface, the settling rate continued to decrease until this rate reached zero at the ultimate concentration. (This change in subsidence rate is, of course, continuous, not discrete.) The paths of typical concentration bands were shown in the region bounded by BOC. These were straight lines representing the constant velocity of concentration bands between the initial and the ultimate concentration, originating at the bottom and terminating at the interface.

Kynch also showed that the batch flux plot, G vs. C, could have several possible shapes, depending on the nature of the material under consideration. Only experimental studies can show the actual shape of the flux plot, but some general rules can be made.

The settling velocity tends to a finite value, the Stokes' velocity, at infinite dilution and since the flux is the product of velocity and concentration, the flux plot must pass through the origin. The flux must also become zero at the ultimate concentration (i.e. the "packed-bed" concentration, C_p) since no further settling is possible. Between these limits the flux is always positive and must therefore pass through a maximum. The curve could be everywhere concave (no inflection points) or, as shown in Figure 2.5, have two inflection points. In some cases the plot could exhibit one (or perhaps three) inflection points and asymptotically approach zero at the ultimate concentration.

If the hindered settling velocity is a function only of concentration it should be possible to represent this function analytically.

The terminal velocity of a rigid sphere falling under the force of gravity is given by Stokes' Law:

$$v_s = \frac{(\rho_s - \rho) g D_p^2}{18 \mu} \quad \ldots \quad (10).$$

where: v_s is the terminal settling velocity (Stokes' velocity),

ρ_s is the partial density,

ρ is the liquid density,

g is the gravitational force,

D_p is the particle diameter, and

μ is the liquid viscosity.

This relation is valid for Reynolds Number, N_{Re}, less than 1.0; i.e.,

$$N_{Re} = \frac{D_p v \rho}{\mu} < 1.0 \ .$$

For non-spherical particles it may be necessary to incorporate a shape factor but the single particle velocity can usually be evaluated with some confidence.

It should be possible to express the hindered settling velocity, v_H, in the form:

$$v_H = v_s f(1 - \epsilon)$$

where: $1 - \epsilon$ is the volume fraction of solids.

If the expression is to be valid over the entire range of concentration,

$$f(0) = 1.0, \text{ and}$$

$$f(1 - \epsilon_p) = 0 \ .$$

where, $(1 - \epsilon_p)$ is the "packed bed" solids fraction.

Note that: $(1 - \epsilon_p) < 1.0$ since the void volume at the ultimate concentration must be filled by the liquid. (For example, the theoretical limit for a packed bed of uniform spheres is $(1 - \epsilon) = 0.74$.)

Several authors have presented empirical or semi-theoretical correlations of this type which, although they might not be valid for the entire range of $1 - \epsilon$, are reasonable approximations of the system studied in each case. Table 2.1 lists typical correlations which have been given by: Steniour (1944); Brinkman (1947); Vand (1948); Richardson and Zaki (1954); and Oliver (1961).

For the case of uniform, rigid spheres that do not interact physically (e.g. flocculate) the settling velocity has been predicted theoretically by Happel (1958). This technique, called the "cell model", surrounds each particle in the system with a spherical cell of liquid and "looks at" the single particle as it settles. (See also, Happel and Brenner (1965), p. 4 and p. 389.)

To this stage the velocity of all particles in the slurry has been considered relative to a fixed co-ordinate system. For the limiting case at infinite dilution, Stokes' velocity, the velocity of a single particle relative to the container walls equals the velocity with respect to the fluid. However, as a slurry settles towards a fixed boundary (the bottom of the cylinder) there must be a "return flow" of fluid because of the volume displaced by the settling solids. The relation between the two velocities can be found easily.

The argument here follows that of Oliver (1961). If the slurry settled at a velocity, v_H, relative to the container walls, the volumetric downward flux, $v_H(1 - \epsilon)$, must equal the volume flow upward of the fluid. At any cross-section the area available for this liquid flow was ϵ so the "return velocity" was;

$$\frac{v_H(1 - \epsilon)}{\epsilon},$$

Table 2.1

Source	$v_H = v_s f(1 - \epsilon)$
Steinour (1944)	$v_H = v_s \, \epsilon^2 \exp\left[- 4.19(1 - \epsilon)\right]$
Brinkman (1947)	$v_H = v_s \left[1 + 0.75(1 - \epsilon)\left(1 - \sqrt{\frac{8}{(1 - \epsilon)} - 3}\right) \right]$
Vand (1948)	$v_H = v_s \, \epsilon^2 \exp\left[\frac{- 2.5(1 - \epsilon)}{1 - 39/64(1 - 2)} \right]$
Richardson and Zaki (1954)	$v_H = v_s \, \epsilon^{4.65}$
Oliver (1961)	$v_H = v_s \left[(1 - 2.15(1 - \epsilon)) \, (1 - 0.75(1 - \epsilon)^{.333}) \right]$
Happel (1958)	$v_H = v_s \left[\frac{3 - 4.5(1 - \epsilon)^{.333} + 4.5(1 - \epsilon)^{1.67} - 3(1 - \epsilon)^2}{3 + 2(1 - \epsilon)^{1.67}} \right]$

and the velocity of the particles with respect to the fluid, v_F, was then;

$$v_F = v_H + v_H\frac{(1 - \epsilon)}{\epsilon}$$

or,

$$v_F = \frac{v_H}{\epsilon} \qquad \ldots (11).$$

2.2 Continuous Settling

The objective of an understanding of batch settling is normally to facilitate design of continuous sedimentation units. A simplified sketch of a continuous settler is shown as Figure 2.6. The feed slurry enters the center of the tank and is distributed over the cross-sectional area. Solids settle and are withdrawn in the concentrated underflow and the clarified liquid overflows at the top. In most cases a slowly moving rake is provided at bottom to aid the removal of settled solids. Although circular tanks will be discussed here, rectangular units are quite common with feed at one end and removal of clarified overflow at the other end. Many other geometrical changes are also found but these change the nature of the problem only in detail. The main design criterion is the size of the settling basin; i.e., the area and depth, but other factors also affect the performance of the settler: rake size and speed, feed distribution, hydraulic flow pattern, and overflow arrangement to name a few.

Coe and Clevenger (1916) not only provided the first analysis of batch settling, but also gave the first design procedure for continuous settlers. The derivation of this technique was based on an intuitive understanding of the physical phenomena but the result is the same as the more rigorous developments which have been given since that time. These authors described how solids pass from one layer to the one below, displacing liquid upward, and then to the next layer until the concentration increased

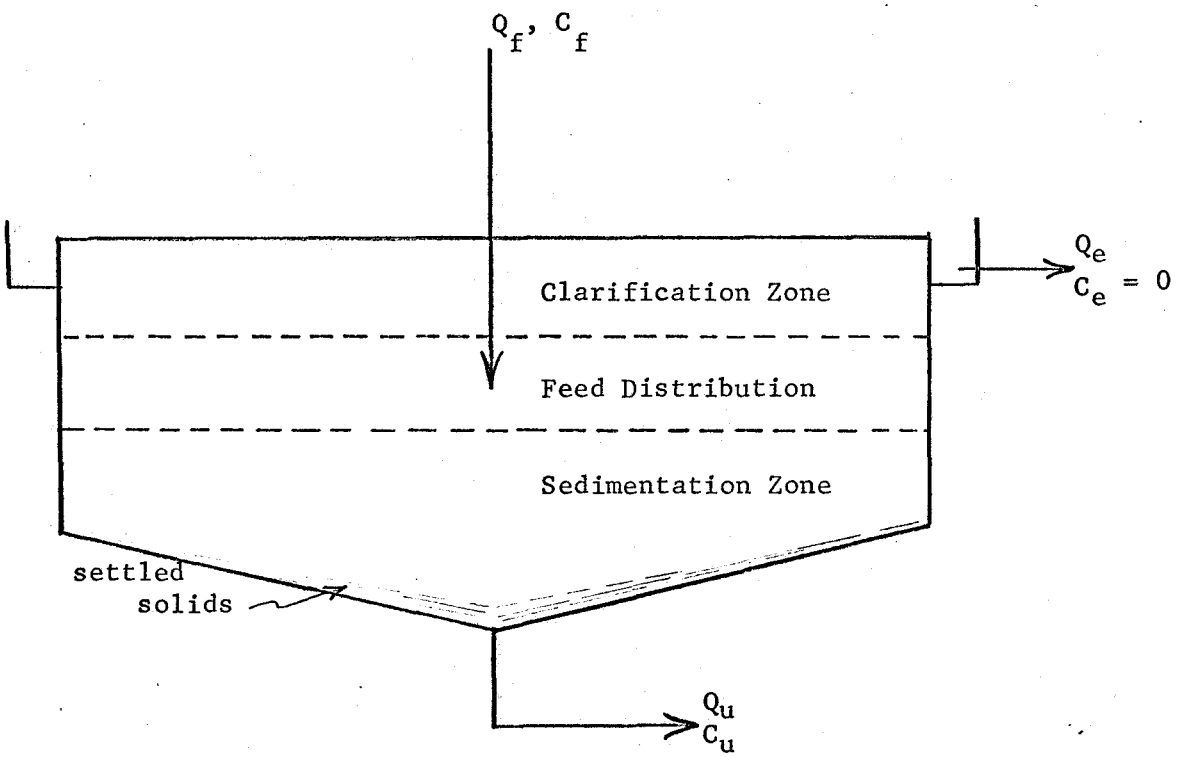

Q is volumetric flow rate
C is concentration of solids

subscripts: f - feed
u - underflow
e - overflow

Figure 2.6

Continuous Settling Unit

from the feed concentration to that of the underflow. By a series of batch settling tests they stated it would be possible to evaluate the "solids handling capacity per unit area" at each concentration. Then it would be necessary to provide the continuous unit with the settling area determined by the lowest value of the "solids handling capacity" over the range of concentration between the feed and the underflow.

A more rigorous development of this concept can be obtained from the liquid and the solids material balance. The material balance for the liquid is;

$$Q_f + Q_e = Q_u \qquad \ldots (12),$$

and for the ideal settler with $C_e = 0$ the solids balance is;

$$Q_f C_f = Q_u C_u \qquad \ldots (13).$$

Also, as the weight of "liquid in" is equal to the weight of "liquid out",

$$Q_f(\rho_f - C_f) = Q_e\rho_e + Q_u(\rho_u - C_u)$$

where: ρ_f and ρ_u are the slurry densities of the feed and underflow, respectively.

Substituting for Q_u by (13) gives:

$$Q_e\rho_e = Q_f C_f\left[\frac{\rho_f}{C_f} - \frac{\rho_u}{C_u}\right] .$$

In most cases $\rho_e \simeq \rho_f \simeq \rho_u$,

then, $$Q_e = Q_f C_f\left[\frac{1}{C_f} - \frac{1}{C_u}\right] .$$

Dividing both sides by the cross-sectional area, A, and noting that Q_e/A at each concentration, C_i, must be limited by the corresponding settling velocity, v_i, if the solids are not to "wash out" in the overflow:

$$\frac{Q_f C_f}{A} = \frac{v_i}{\left[\frac{1}{C_i} - \frac{1}{C_u}\right]} \qquad \ldots (14).$$

Note also that;

$$\frac{Q_f C_f}{A} = \frac{Q_u C_u}{A} = G$$

or, at steady state the solids flux is constant throughout the unit. If the solids flux is evaluated over the desired range of concentration using equation (14) with the values for $v_i = f(C_i)$ obtained from the batch tests, the area requirement for the settler may be based on the limiting (lowest) flux value over this range. This procedure gives the result,

$$G_{min} = \frac{v_L}{\left[\frac{1}{C_L} - \frac{1}{C_u}\right]} \quad \ldots (15).$$

where: G_{min} is minimum solids flux per unit area between C_f and C_u, and

v_L is the settling velocity at the limiting concentration, C_L.

Equation (15) is the design equation given by Coe and Clevenger, but in a slightly different, though equivalent, manner than in the original work (1916).

The analysis of batch settling given by Kynch (1952) has been extended to apply to continuous settling by Talmage and Fitch (1955). These authors have shown how a single batch test could be used to obtain the necessary $v_i = f(C_i)$ relation. They started from Kynch's result that;

$$u = -\frac{dG}{dC} \quad \ldots (9),$$

is the constant, upward velocity of a concentration layer originating at the bottom and terminating at the interface which moves downward with velocity, v. All particles in the system must have passed through this layer by the time it reached the interface. The total mass of particles in

the system was;

$$C_o z_o A$$

where: C_o is the initial concentration,

z_o is the initial depth, and

A is the constant, cross-sectional area.

If a layer of concentration C_i reached the interface at time t_i, the mass of particles which "passed through" this layer was the total mass of solids in the slurry:

$$C_o z_o A = C_i t_i (v_i + u_i) A$$

and since $(v_i + u_i)$ was constant;

and $$u_i = \frac{z_i}{t_i} .$$

Combining the two equations gave,

$$C_i = \frac{C_o z_o}{v_i t_i + z_i} \qquad \ldots (16).$$

Referring to Figure 2.7 it can be seen that $v_i t_i + z_i = z_i^*$, the intercept at t = 0 of a tangent to the interface vs. time curve at (z_i, t_i). This value, z_i^*, is the depth of the slurry if it were at a uniform concentration, C_i. Using equation (16) with the interface vs. time curve from a single batch test at the feed concentration, the values for $v_i = f(C_i)$ could be determined. The results were then used in equation (14) to evaluate the minimum solids flux.

Another graphical technique that can be used to determine the limiting solids flux which must be used in determining the required settler area has been described by Tory (1961) and Robins (1964). A batch flux plot is shown in Figure 2.8. This curve can be constructed using either a series of batch tests (Coe and Clevenger (1916)) or from a single test at

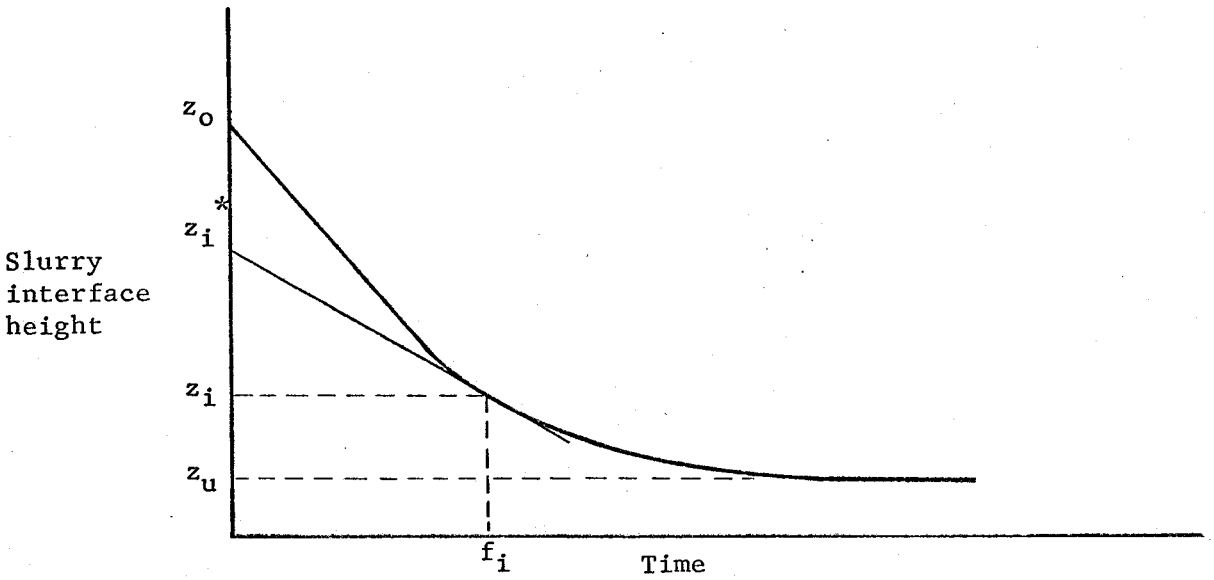

Figure 2.7

Talmage and Fitch Construction

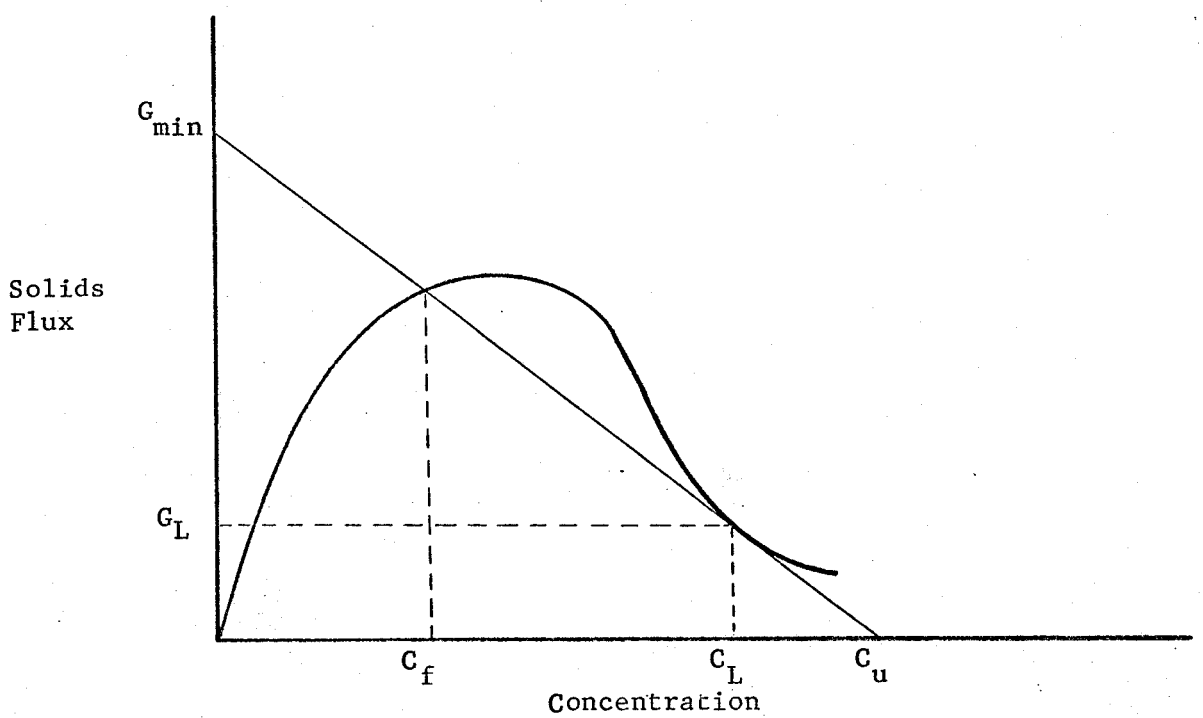

Figure 2.8

Batch Flux Plot Construction

the feed concentration (Talmage and Fitch (1955)). A line was drawn through the desired underflow concentration, C_u, tangent to the flux curve. The intersection of this line with the ordinate was the minimum solids flux, G_{min}, which was used in the design equation (15) to determine the settler area. By similar triangles on Figure 2.8,

$$\frac{G_{min}}{C_u} = \frac{G_L}{C_u - C_L}$$

and substituting, $G_L = v_L C_L$

$$G_{min} = \frac{v_L}{\left[\frac{1}{C_L} - \frac{1}{C_u}\right]} \qquad \ldots (16),$$

which is the original design equation based on the limiting solids flux concept.

This information can be used to construct a "continuous flux plot". The solids flux in a continuous unit results from two components: the settling rate of the solids and the downward movement of the slurry due to the underflow rate. Therefore;

$$G = C(v + V)$$

where $V = \frac{Q_u}{A}$, the velocity resulting from the downward flow of the slurry.

The flux in a continuous settler must be constant so,

$$G_{min} = G_u = \frac{C_u Q_u}{A} ,$$

or,

$$V = \frac{G_{min}}{C_u} .$$

At the limiting solids concentration,

$$G_{min} = C_L \left[v_L + \frac{G_{min}}{C_u} \right]$$

or,

$$G_{min} = \frac{v_L}{\left[\frac{1}{C_L} - \frac{1}{C_u} \right]} \quad \ldots (16),$$

which is again the same result. This continuous flux plot, shown as Figure 2.9, is constructed by adding to the batch flux the flux component resulting from the slurry flow at each value of concentration. This plot is, of course, valid only for the underflow rate selected in making the plot.

It has been shown that these design procedures are based on the same premise: that the required settler area is determined by the limiting solids flux.

In summary the Coe and Clevenger method utilizes a series of batch tests at several values of initial concentration to determine the limiting "solids handling capacity". Talmage and Fitch have shown how a single batch test at the feed concentration could be used to evaluate the necessary $v_i = f(C_i)$ relation over the range of concentration from the feed to the underflow. The flux plot methods are graphical techniques to determine the minimum continuous flux for any desired underflow concentration. The most widely used method is to use a series of batch tests to construct the batch flux plot and determine G_{min} by selecting a value of C_u.

To this point the area requirement considered has been only that for the solids zone in the sedimentation basin. In some cases the limiting factor in design could be the clarification capacity. If the upflow velocity (Q_e/A) in the clarification zone exceeds the terminal settling

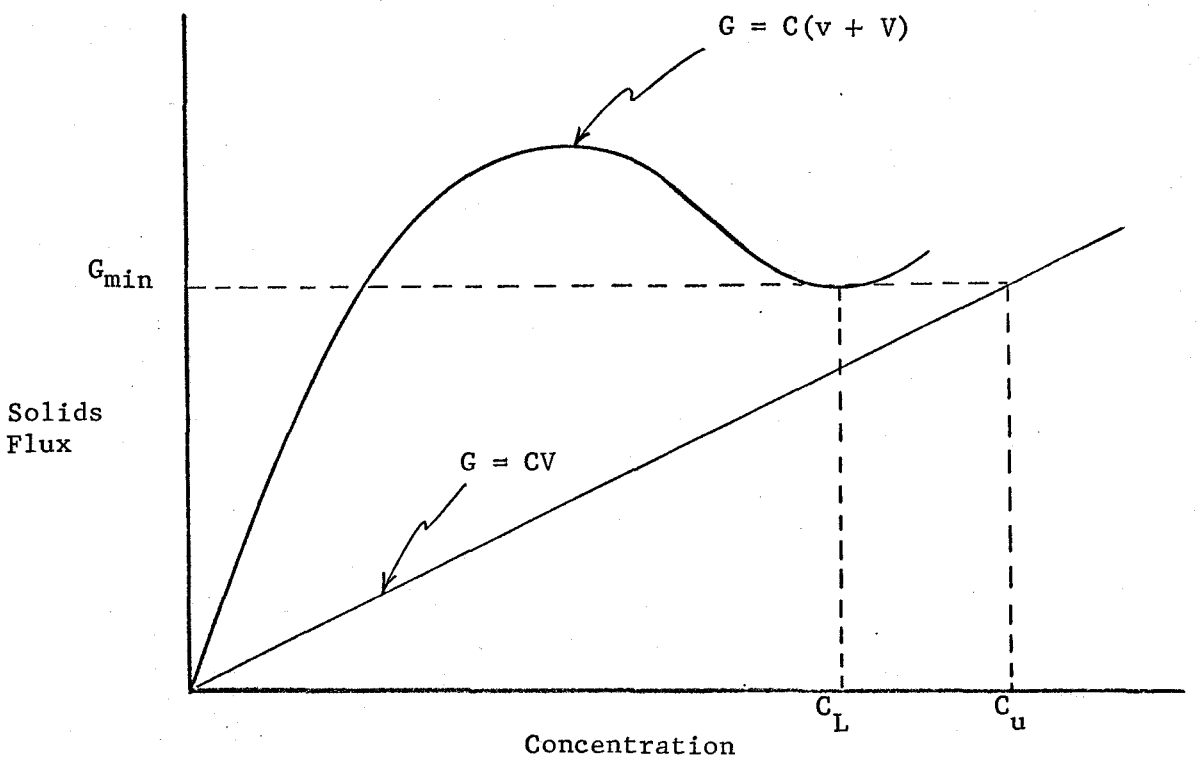

Figure 2.9

Continuous Flux Plot Construction

velocity of a particle, that particle will be carried out in the overflow. Some material might always be restricted by this consideration; i.e., the solids limiting flux cannot be reached before the upflow velocity exceeds the Stokes' velocity of a significant fraction of the feed particles.

The above analysis of a continuous settler has not considered the depth requirement and, in fact, the settling rate appears to be truly independent of depth. For discrete particles this is a reasonable conclusion but for particles which interact in any manner during the settling process the depth of the continuous unit is an important design parameter. In some applications it could be necessary to provide adequate depth for short-term storage capacity of sludge. In biological processes; such as the activated sludge process, the detention time, and therefore the depth, must be held to a low enough value to prevent the solids from becoming anaerobic.

The determination of the depth of a settling basin for compressible slurries has been given by Roberts (1949). This method is, at best, an approximation but it does provide some rationale in the selection of the depth requirements of the compression zone. Roberts assumed that the depth of the compression zone in the batch test was a function of time in the form:

$$\frac{dz}{dt} = k(z - z_{\infty})$$

where: z is the depth of the compression zone at time t, and

z_{∞} is the ultimate depth of the compression zone at $t = \infty$.

This equation was integrated to give;

$$\ln \frac{z - z_\infty}{z_c - z_\infty} = kt \qquad \ldots (17)$$

where: z_c is the depth of the compression zone at the critical point, and

$t = 0$ at the critical point.

In many cases z_∞ was not known so it was necessary to estimate this value and to test the estimate by plotting equation (17) on semi-log axis. If a straight line resulted the slope was k and if not a new estimate was made for z_∞. The depth of the compression zone was related to the concentration by,

$$C_i = \frac{C_o z_o}{z_i} \qquad \ldots (18).$$

Using equation (17) it was then possible to evaluate the time required for the accumulated solids to compact from the critical value to the desired underflow concentration. Knowing the underflow rate and the settler area the depth of the required compression zone was then calculated. To this value it is common practice to allow 2 to 5 feet for feed distribution, bottom slope and clarification zone.

2.3 Experimental Studies

There is a large volume of literature on hindered settling of many different types of material. The most meaningful studies have measured the transient concentration profile of batch settling tests, not only the rate of fall of the interface, but also the changing concentration gradient below the interface. Attempts to sample below the surface of the slurry have not been very successful as each measurement disturbs the system. Several important studies have been reported using transmittance of

radiation to measure internal concentration gradients.

Fuenstenau (1960) developed an X-ray transviewer to observe concentration profiles during batch sedimentation of a flocculated kaolin slurry. Tory (1961) used gamma-ray absorption to study batch settling of a calcium carbonate slurry. Work by Cole (1968) with the specific objective of evaluating the Kynch theory employed Tm^{170} gamma radiation to detect concentration changes during sedimentation of a kaolin clay, Hydrite MP. These studies were very similar in scope and all concluded that the Kynch analysis described batch settling very well at lower concentrations. The settling rate appeared to be a function only of concentration and the concentration "bands" were observed as they moved from the bottom of the vessel to terminate at the interface. Also, a single test could be used to evaluate the settling rates at different concentrations as predicted by Talmage and Fitch (1955). However, at the higher concentrations this simple analysis did not completely explain the observed phenomenon. In the extremely hindered case, settling by compression, Fuenstenau (1960) found that the settling rate could be best explained by considering the rate of elimination of water through small channels in the void volume of the settling mass. This fact cannot be considered a deviation from the Kynch theory since during the compression stage the particles are actually resting one upon the other and further compaction occurs as the weight of this bed "squeezes" the water out of the underlying voidage. Also, the material used in each of these studies had a strong tendency to flocculate so at the higher concentrations this might be expected to be the dominant factor controlling the settling rate.

It must be remembered that the Kynch theory employs a model that considers each particle to retain its individuality (discrete particles)

and the particles are not actually in contact (except, perhaps, random collisions). Cole (1968), in fact, attempted to apply the Kynch analysis to the settling of activated sludge, a biological sludge with a density only slightly greater than that of water and a very strong "flocculating" characteristic. Except at very dilute concentrations this material settles entirely by a compaction mechanism.

Shannon and Tory (1965) reported settling studies with spheres of a relatively uniform size. This material was selected to conform as closely as possible to the idealized model; i.e., discrete particles which settle to an incompressible layer on the bottom. The results were in very close agreement with the theory.

Only very few studies are found in the literature describing the operation of a bench or a pilot scale continuous settler. Comings (1940) and Comings et. al. (1954) have reported an experimental study employing an 8 inch diameter continuous apparatus used in thickening a calcium carbonate slurry. These workers attempted to relate the operation of the continuous unit to batch studies by a "Coe and Clevenger-type" approach with very little success. The controlling factor in the performance of the thickener appeared to be the compression zone so the effect of detention time and the rake action were most important. Attempts to re-evaluate the data using the "flux plot" concept are no more successful.

Scott (1968a) and (1968b) has reported a very extensive study using a 6 ft. diameter pilot-scale thickener to separate a flocculated kaolin slurry. The relevant batch tests were analyzed by the Coe and Clevenger approach, the Talmage and Fitch technique and the flux plot construction. For this study the Talmage and Fitch graphical determination of required thickener area gave the best comparison to the actual settler performance.

No really satisfactory explanation was given for this result. It was suggested that the settling rate at the higher concentrations was unrealistically large due to channeling during the compression period. This would lead to an underestimate of the required thickener area. The author also suggested that the design technique based on the single test (at a lower concentration) would give more reasonable settling rates since these channels did not have time to form. Perhaps in this study also, the dominant mechanism was the rate of compaction, so the limiting factor was the compression zone or the rate of flocculation.

These studies show that no truly satisfactory design procedure is available. The information cited here neither confirmed nor defied the Kynch analysis *per se*. The conclusion must be that when the slurry conforms to the restraints of the model the developed theory is quite satisfactory but in many (perhaps most) cases the material is so unlike the idealized description that other factors must be incorporated into the design procedure.

CHAPTER 3

EXPERIMENTAL APPARATUS AND PROCEDURE

The previous discussion has described the theoretical aspects of sedimentation and the somewhat idealized model on which analysis is based. The apparatus and experimental methods used in this work were designed in light of this theory and will be described here.

3.1 Batch Studies

3.1a Apparatus

The requirements for a vessel to study batch settling rates are relatively few. Commonly, a glass cylinder such as a 2-liter graduate is used. For a meaningful study the diameter of the column must be large enough to justify ignoring the wall effects. Cole (1968) measured initial settling velocities of a kaolin clay in 2", 4", 6", 8" and 12" diameter columns and found very little effect. He noted a slight increase in initial rate in the 2" column at the lower concentrations. Cole also measured the initial settling velocities at several different initial depths of slurry. As expected by the theory for discrete particles, the initial depth of the slurry is not important. Since transparent acrylic resin tubes were conveniently available with 7.6 cm (3.0" nominal) inside diameter these were chosen. The overall length of the column was 4.5 ft. to provide for a 100 cm initial depth of slurry and allow additional height for mixing. At the base of the column a flange was cemented in place to receive a flat disc held in place by machine bolts and wing-nuts.

Originally, it was intended to use a photo-extinction technique to observe both internal concentration gradients and the rate of fall of the liquid-slurry interface. The nature of the particles used was such that only at the very high solids concentrations could a true interface be observed and except for the dilute slurries the system was essentially opaque to the light source. This method did provide a successful technique to observe the rate of fall of the "interface" by defining "interface" as the light intensity corresponding to any pre-selected value of solids concentration.

Light intensity was measured by selenium photo-voltaic cells mounted at one end of an opaque cylinder with an optical slit (1 cm wide) at the other end. Nine photo-cells were mounted against the outside of column at 10 cm increments. The outside of the settling column was masked except for 1 cm wide bands at each 10 cm increment. The photo-cells were positioned diametrically opposite to the light source. The light source consisted of two standard 4 ft. fluorescent light tubes mounted vertically against the side of the column. This light source yielded as high an intensity of light as the incandescent bulbs tried and did not radiate as much heat to the slurry. In this way the concentration of particles could be measured at nine positions in the settling column.

A drawing of the apparatus used for the batch settling studies is shown as Figure 3.1.

By observing the output of each photo-cell continuously or at known time intervals, the concentration at each vertical position (10 cm increments) could be evaluated. Since continuous monitoring of nine signals was not practical, a digital data logging system was used to record data.

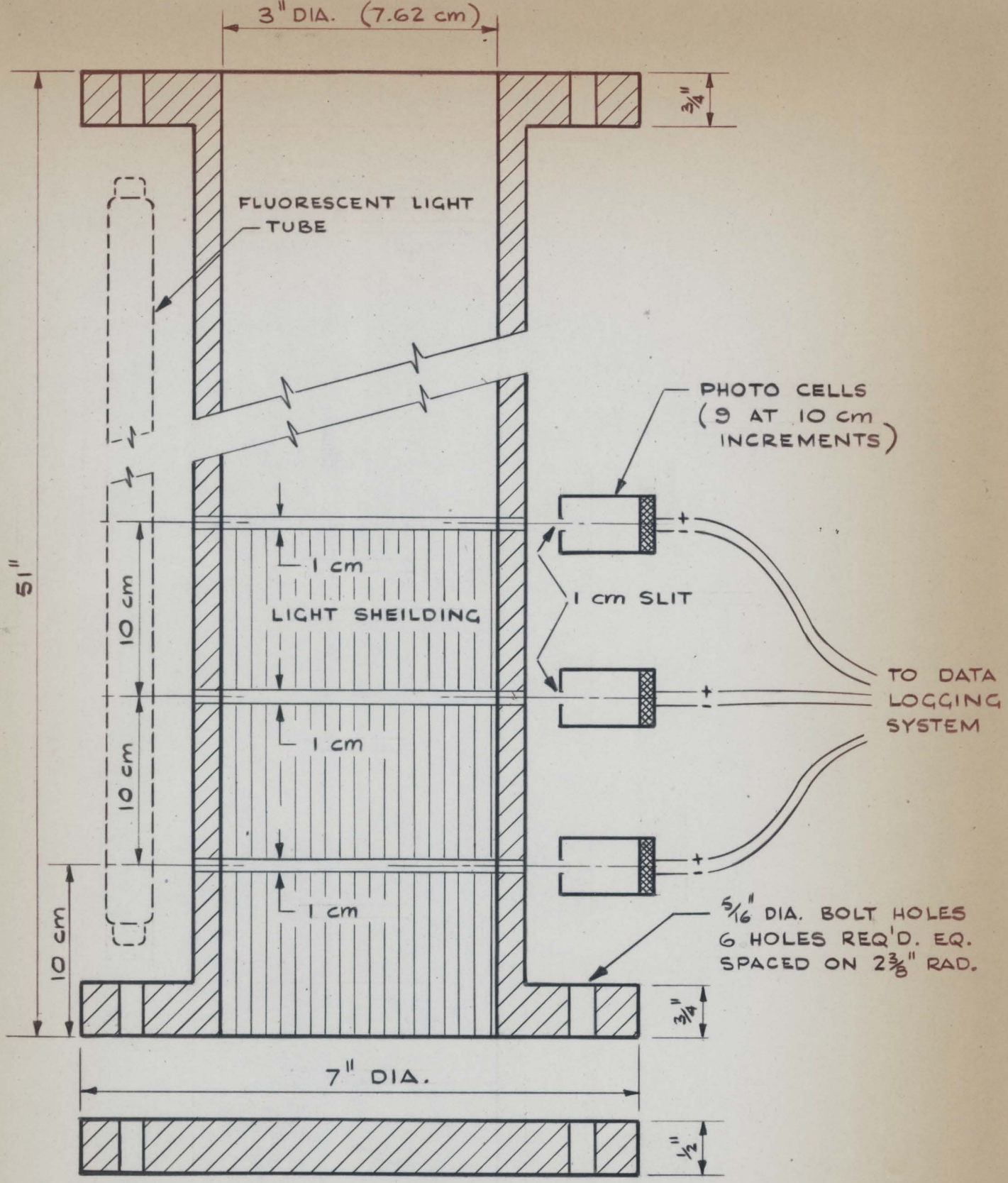

FIGURE 3.1
DRAWING OF BATCH SETTLING COLUMN

This unit electronically sampled each photo-cell at pre-selected time intervals and recorded the information on magnetic tape.

A schematic of the batch settling experimental system is shown in Figure 3.2.

3.1b Description of the Digital Data Logging System

The system consists of four integrated devices to measure several input signals and record the information on magnetic tape.

(1) Crossbar Scanner (Model 707-120)

This device is essentially a multiplexer that selects which input channel to "look at" and routes the information to an encoding device. The unit has the capability of scanning up to 60 "two-wire" inputs in a single-step, semi-continuous or continuous mode in a sequential or an externally controlled scanning sequence. Scanning rate of up to 30 channels per second are possible.

(2) Digital Multimeter (Model 6305)

Information from the scanner is converted from an analog to a digital signal and displayed on five digital read-out tubes. The multimeter may be used to indicate; d.c. voltages from 0.001 mv to 750 volts; frequency in the range 10 cps to 1 mc; or time intervals from 0.001 milliseconds to 10 seconds. Visual display also includes symbols to indicate the mode of operation selected.

(3) Output Control (Model 825E)

This device receives digital information from the digital multimeter and encodes the signals as seven-level, BCD (binary coded decimal)

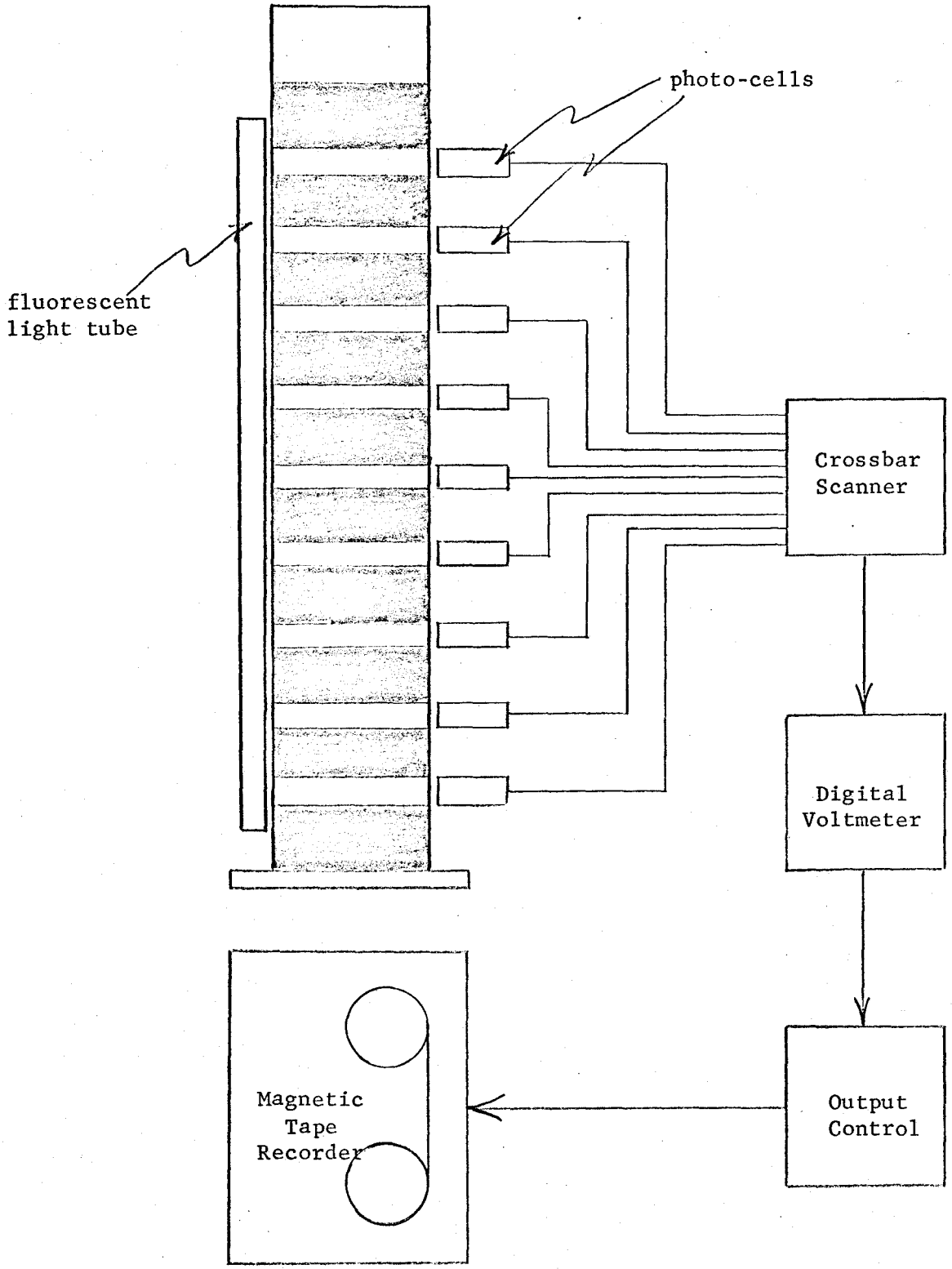

Figure 3.2

Batch Settling Experimental System

characters to be recorded on magnetic tape. Each input channel is coded as a 10 character BCD word for conventional seven-track magnetic tape recorders. Each word is separated by a word separator code (decoded as a "blank"). After the number of channels scanned as one record (as selected by the scanner) the output control generates an "end-of-file" signal.

A sample format for one word representing a reading of +121.5 mv on channel number 3 (after decoding the BCD information) is given here:

b003+121505

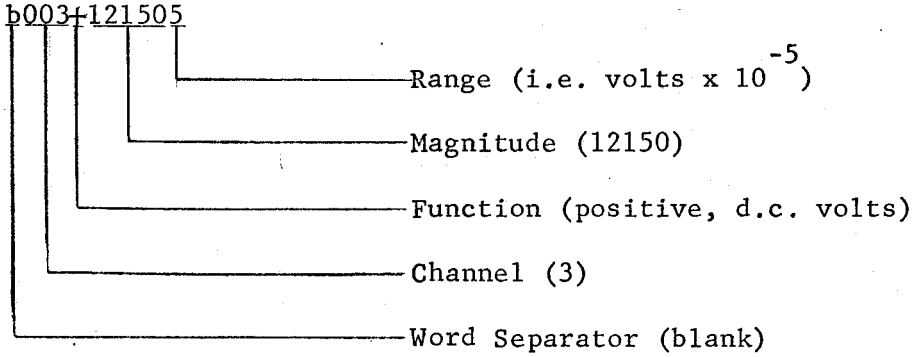

(4) Incremental Digital Recorder (Model 6200)

The information from the output control is recorded on seven-track, ½ inch magnetic tape at a density of 200 bpi ("bits per inch"). Tape motion is provided by two opposed torque motors ("tape-up" and "supply") and a light source-photo cell system detects reflective markers or tape breaks. Up to 1200 ft., IBM compatible tapes may be used.

All four units are housed in a single cabinet with a power cable and an "on-off" indicator lamp.

3.1c Experimental Procedure

The particles chosen for this study were polystyrene spheres from the Dow Chemical Co. The particles were near-perfect spheres with a mean diameter of 285 microns and density of 1.044 gm/cc. (A more complete description of this material is found in Section 3.3.) They were chosen

to conform as closely as possible with the mathematical model of settling.

The column was filled to a depth of 100 cm with distilled water and surfactant (a liquid soap) was added in a concentration of 1 ml/lit which reduced the surface tension to approximately 35 dynes/cm^2 as measured by a Du Nouy ring surface tensiometer. It was necessary to reduce the surface tension since the polystyrene was very poorly wet by pure water. The column was allowed to stand for at least 24 hours to allow the system to come to thermal equilibrium (occasional checks of the liquid temperature indicated $30^{\circ}C$ with fluctuations of $\pm 2^{\circ}$ over the entire experimental period).

A weighed amount of particles was added to the column and the slurry repeatedly mixed to ensure wetting of all spheres. This procedure caused some foam formation resulting from the surfactant so time was allowed for the foam to break and gentle surface mixing usually forced the remaining particles into the liquid. With the particles settled the liquid level was lowered to the 100 cm mark by pipetting out the amount of supernate displaced by the volume of solids added. In this way the initial depth of slurry was always 100 cm and the initial concentration could be evaluated knowing the amount of solids added and the volume of the slurry in the column.

The nine photo-cells were connected to input channels one through nine of the data logging systems which was setup in the continuous mode to scan channels zero through ten. This was done to write a dummy word at the beginning and end of each record. The scanning rate was selected by consideration of the length of experimental run and was determined by measuring the length of time required for the scanner to sample 100 channels. The scanning rate in each case had to be sufficiently slow to allow time for

the tape drive to move through a 3.4 inch "end-of-file" gap between channels ten and zero. The fastest scanning rate used, at the dilute concentrations, sampled each channel four times per minute and the slowest rate was 1.75 times per minute.

The slurry was thoroughly mixed by hand and the data logging system enabled to start a run. The light intensity initially corresponded to the transmittance at that concentration and after all particles had settled, corresponded to zero concentration. In most cases each settling test was done in triplicate.

This procedure was repeated to cover the desired range of initial concentration. Relatively small concentration increments were made in the first few runs to give the light-intensity-concentration relation, and when it became apparent that the light did not penetrate the slurry larger increments were used. (Note that at the higher concentrations the bottom photo-cells might never be exposed to the light because the particles accumulated on the bottom obscurring the light source.)

3.2 Continuous Settler

The object of the study was to construct a continuous settler which when operating under laboratory conditions could be compared with predictions based on the analysis of the batch data. The design was based on the considerations discussed in Section 2 and an effort was made to meet the idealized model as closely as possible.

3.2a Apparatus

The continuous sedimentation vessel was designed similar to the batch column in size with the necessary adaptation for continuous feeding of

slurry and removal of overflow liquid and underflow slurry. The column was, as in the batch tests, 7.6 cm I.D. but a slurry from the feed tank was continuously fed to the center of the vessel and the concentrated underflow was removed at the bottom: both under positive flow control by tubing pumps. The essentially solids free overflow was collected at the top and recombined with the underflow in the feed reservoir to allow continuous operation.

The feed slurry was introduced to the column through a vertical tube, ¼ inch (0.625 cm) I.D., positioned on the center axis of the column. The solids were radially distributed by an impingement baffle on the end of the feed tube 100 cm above the bottom of the column. This provided a clarification zone of 30.5 cm. The feed line was fitted with a valve to direct the entire feed slurry to a sampling port for collecting a timed, volumetric sample which was used to calculate flow rate and feed concentration. The feed was pumped from the reservoir to the feed distributor by a Masterflex tubing pump. The flow rate was controlled by use of an SCR speed controller regulating the pump motor.

A conical bottom for removal of concentrated underflow was held in place by a flange fitted at the base of the column. Since design information on the slope of the bottom referred to tanks provided with moving rakes, a slope of 0.5:1 (vertical:horizontal) was selected. Another tubing pump, similar to the feed pump, removed the underflow slurry at an adjustable flow rate and returned the slurry to the feed tank.

The clarified liquid overflowed through four sharp-edged, V-notch weirs evenly spaced around the top of the column. It was felt that this arrangement would give a relatively uniform flow pattern at the top of the vessel. This overflow was collected in a circular launderer and passed

through a downcomer to be returned, under gravity, to the feed reservoir. The feed tank used had a volume of approximately 17.5 lit and was fitted with a stirrer to keep the particles in suspension.

A drawing of the continuous settler is given as Figure 3.3.

As in the batch studies, it was intended to observe concentration profiles in the sedimentation zone during settler operation. The outside of the column was masked, except for bands at 10 cm intervals where photo-cells were positioned diametrically opposite to the light source: identical to the batch apparatus. The data logging system was used to record the output of each photo-cell.

A schematic of this system is shown as Figure 3.4 and Figure 3.5 is a photograph showing the apparatus setup, but not actually in operation.

3.2b Operation of the Continuous Settler

The apparatus was thoroughly washed and rinsed with distilled water and setup as shown in Figure 3.4. Distilled water was added to the feed tank and pumped to fill the column and surfactant added in a concentration of approximately 1 ml/lit. The desired flow rate of the feed and the underflow pumps was set and the system allowed to run for a day to thoroughly wet all surfaces. Solids were added to the feed reservoir and the surface violently agitated by hand to force the particles into the liquid: once the particles were introduced to the liquid the stirrer maintained a uniform suspension in the feed tank. Each time the unit was started up all particles would slowly accumulate on the bottom of the settler and could be removed by tapping the bottom to start them flowing out the underflow. This could occur several times again for the first few days of operation and then a layer, one or two particles deep, would form in the bottom and no further problems

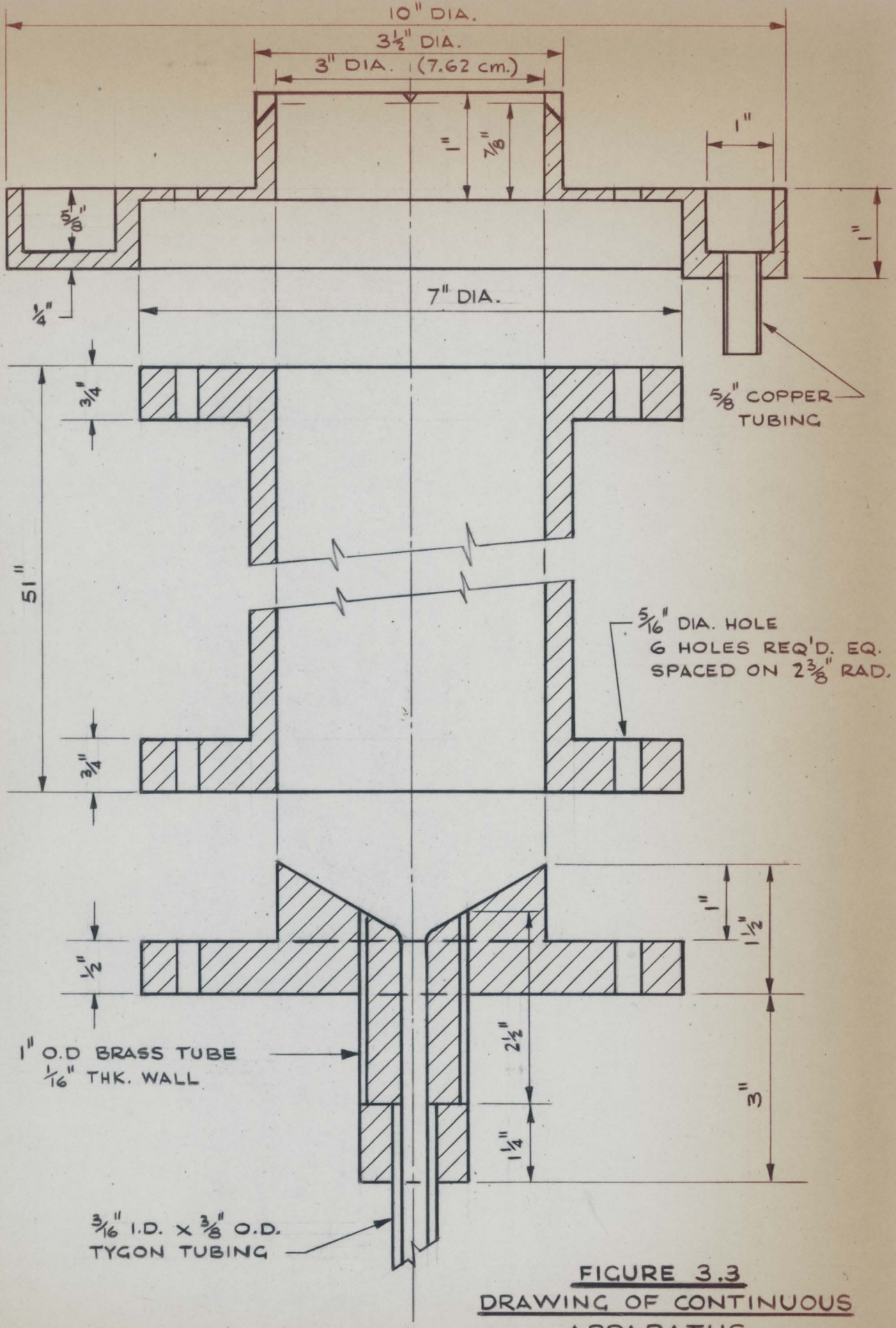

FIGURE 3.3
DRAWING OF CONTINUOUS APPARATUS

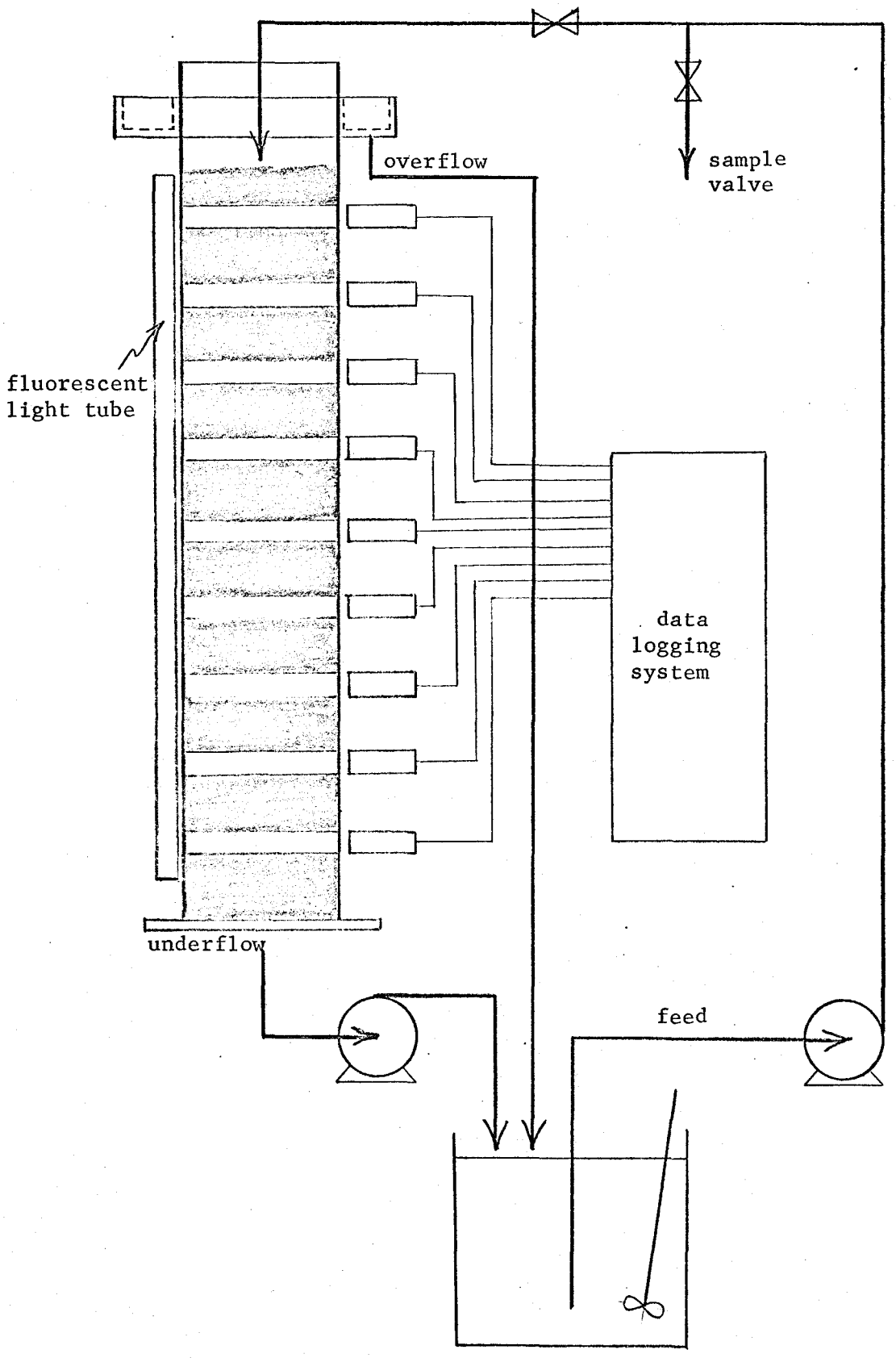

Figure 3.4

Continuous Settling Experimental System

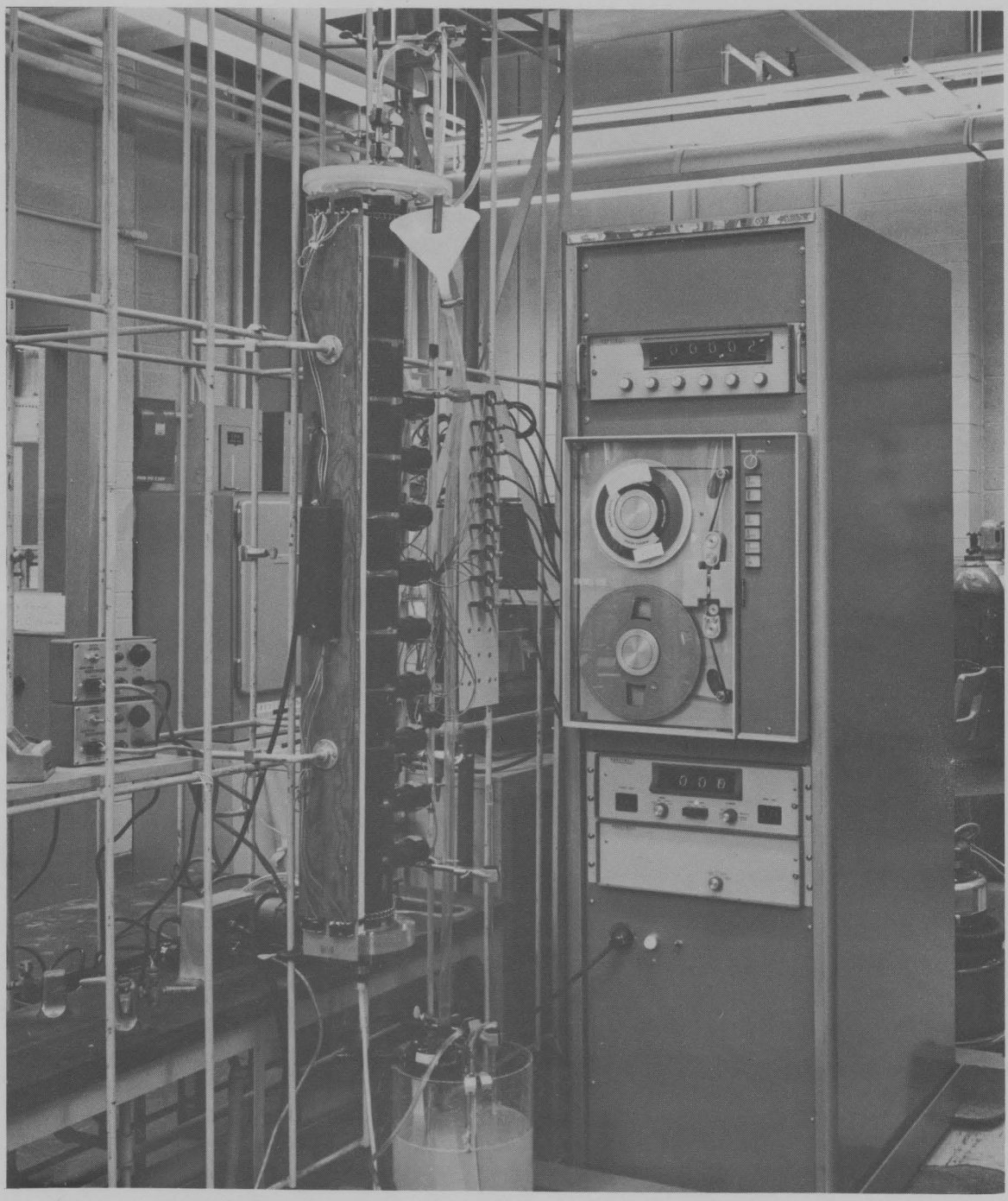

FIGURE 3.5

EXPERIMENTAL APPARATUS

with accumulation of solids would occur. It was also noted that if the underflow pump was operated at too low a rate particles would accumulate on the bottom. The lowest underflow rate which could be used for this reason was approximately 100 ml/min; which is an average liquid velocity along the base of 5 cm/min.

After the unit appeared to have reached steady-state the data logging system was conditioned and used to record the light intensity reading at each photo-cell. The scanner mode was "single scan" and was actuated 25 times to give 25 readings of light intensity at each position. A timed, volumetric sample of the feed, underflow and overflow was collected for flow rate calculations and solids determination by filtering with Gooch crucibles. Sampling the feed slurry caused a small perturbation to the operating conditions since the entire feed stream was diverted for 1½ to 2 minutes. It appeared that the unit steadied out within 15 minutes after this sampling. One hour after the first set of samples the settler was again sampled and if both tests agreed it was assumed that the unit was at steady state: if not, the sampling was repeated an hour later.

The flow rate selected for the underflow was that which could just ensure continuous removal of settled particles as mentioned above. The feed rate was the greatest flow which did not exceed the clarification capacity of the unit. Once selected, these flows were maintained as closely as possible during the entire experimental period. The solids loading was increased by adding more particles to the feed tank.

After two or three successful runs the stirrer was shut off which allowed all particles to settle out in the feed tank. In this way the light intensity corresponding to zero concentration in the settling column could

be recorded. It was necessary to account for the change in the zero concentration light reading in this way since the light transmission through the liquid changed slowly during the experimental period.

3.3 Description of Particulate Solids Used

The type of particulate solids selected for the study was based on considerations of the settling model. The main criteria was that the material not flocculate, but remain as discrete particles in suspension. The material selected was polystyrene spheres called Pelspan 80 manufactured by Dow Chemical Co. as the raw material used in making expanded polystyrene foam. These particles behaved as discrete, rigid spheres in suspension but had some unforeseen disadvantages.

The method of size analysis employed was a photographic technique. A sample of the particles was placed on a translucent plate and photographed at about "times three" magnification. After several such samples were taken, a graduated scale (1 cm, with 0.1 mm divisions) was also photographed at the same degree of magnification. This negative was developed and all exposures printed at the same degree of enlargement on 8" x 10" lightweight paper. A Zeiss Counter was used to count the number of particles in each size interval over the size range of the sample. (The resulting size analysis is shown as a normal probability plot in Figure 3.6.) One of the particle photographs is included here as Figure 3.7.

The particles were found to be very hydrophobic. It was necessary to reduce the surface tension of the water so the sphere would be "wet" by the liquid. Of the several surfactants tried the one selected was a liquid soap for laboratory use (Fisher Scientific Co., Cat. No. SO-F-105). This was chosen on the basis of its low-foaming characteristic. In a concentra-

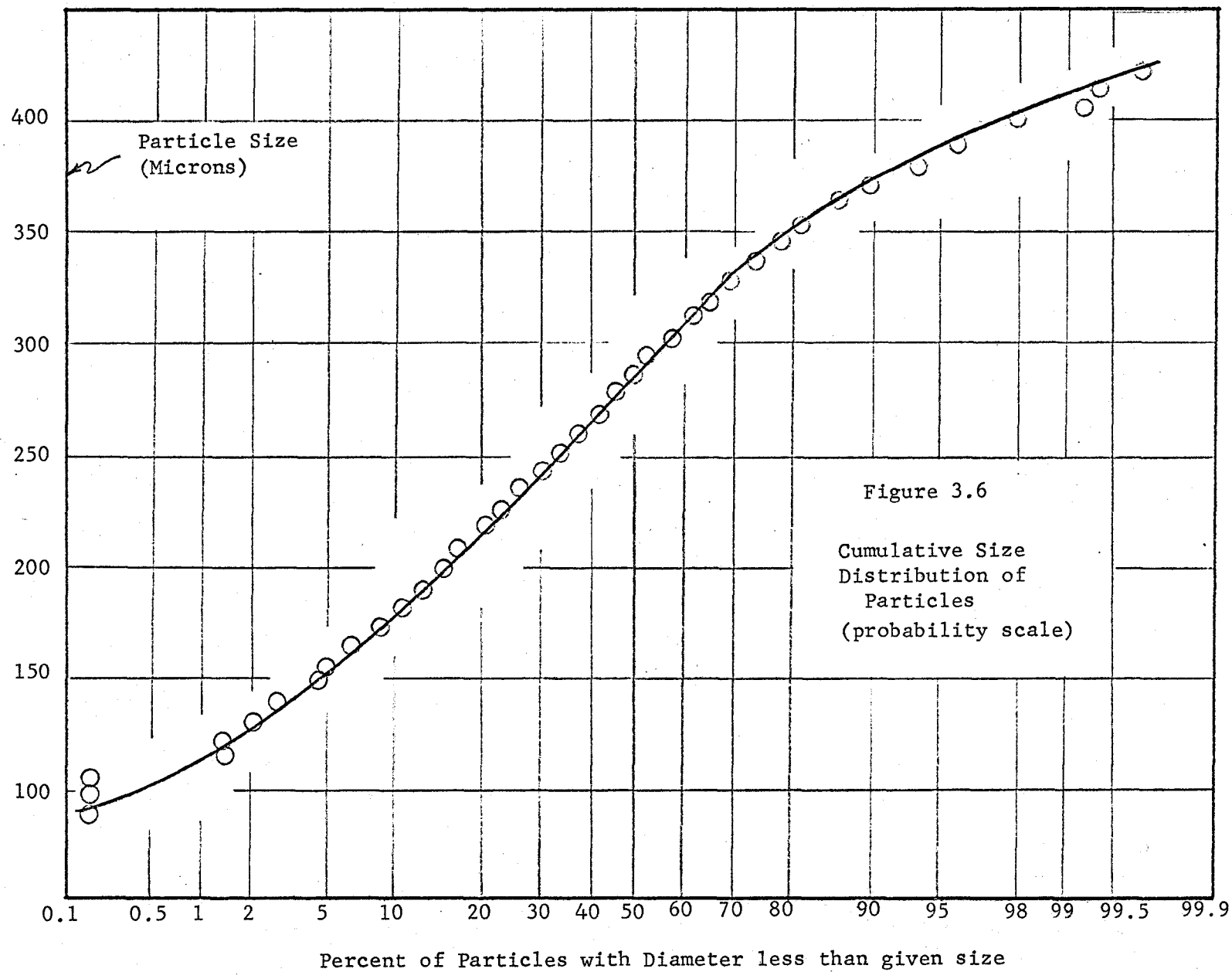
Particle Size
(Microns)
400
350
300
250
200
150
100
0.1
0.5
1
2
5
10
20
30
40
50
60
70
80
90
95
98
99
99.5
99.9
Percent of Particles with Diameter less than given size
Figure 3.6
Cumulative Size
Distribution of
Particles
(probability scale)

Figure 3.6

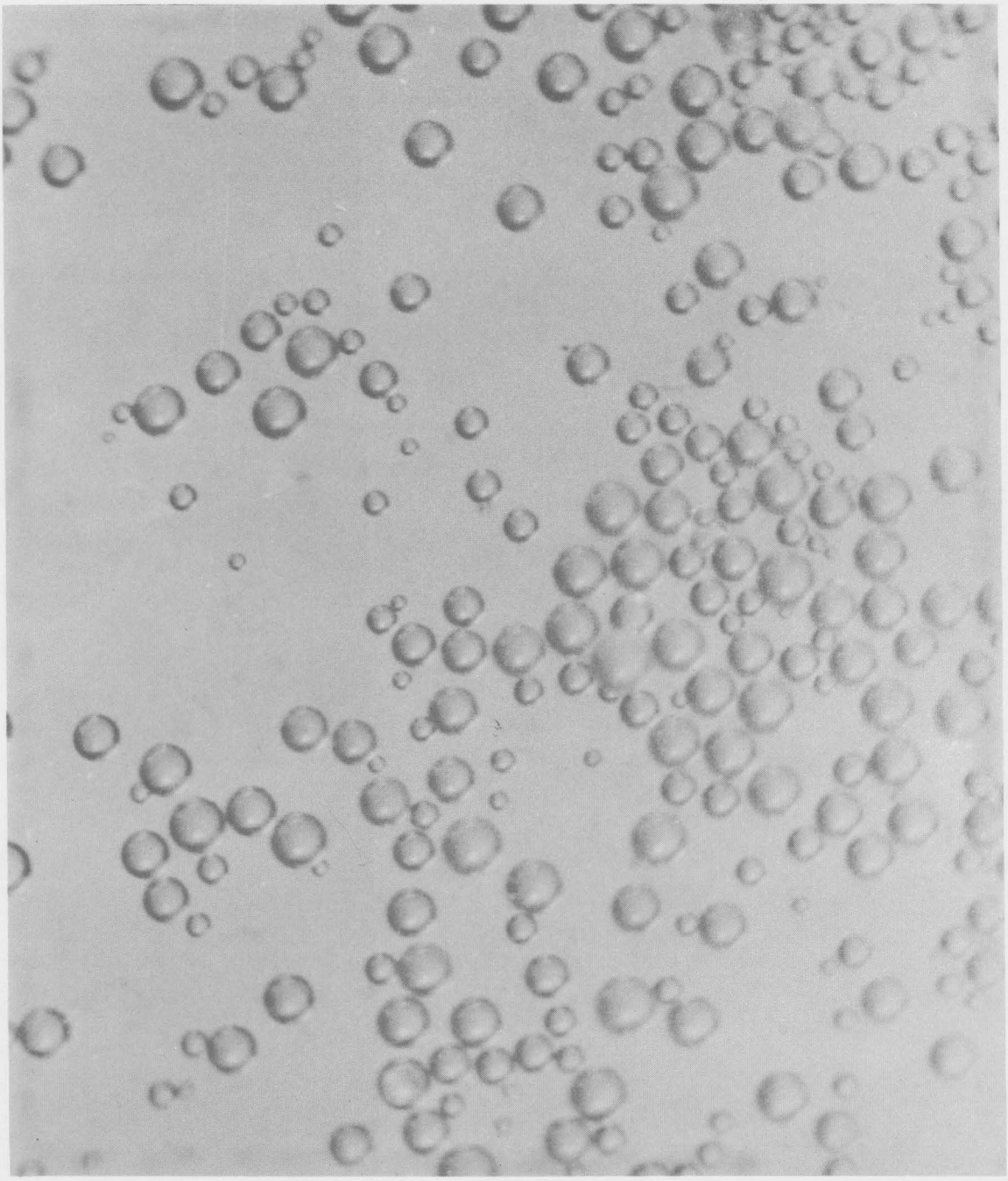

FIGURE 3.7

PARTICULATE SOLIDS USED IN STUDY

tion of 1 ml/lit the surface tension of the water was reduced to 35 dynes/cm^2 as measured by a Du Noüy ring surface tensiometer.

A summary of the physical properties of the liquid and the particles is given in Table 3.1.

Table 3.1

Physical Properties at $30^{o}C$

Physical Property	Value	Method
Liquid Density (ρ)	0.996 gm/cc	weighing bottle compared with standard value.
Solid Density (ρ_s)	1.044 gm/cc	volumetric displacement of known weight.
Viscosity (μ)	0.8007 cp	viscosity tube compared with standard value.
Mean Particle Diameter (D_p)	285 microns	photographic technique.
Standard Deviation of D_p (σ)	$\pm$ 75 microns	slope of probability plot.

CHAPTER 4

EXPERIMENTAL RESULTS AND DISCUSSION

Because the experimental procedure resulted in a large amount of raw data in the form of punched data cards, the results are summarized in Appendix B. The amount of data necessitated the use of a digital computer in all stages of data reduction.

4.1 Batch Studies

Immediately after initial mixing the data logging system was activated to record the light intensity reading of each photo-cell at pre-selected time intervals. The first reading was then the light intensity at the initial solids concentration, assuming that the particles were uniformly distributed. The final reading of each photo-cell, after all particles had settled, gave the light intensity transmitted by the liquid; i.e., zero solids concentration. This value was different for each photo-cell and decreased slowly during the experimental period, presumably due to a slow reaction between the surfactant and the metal ions in the water. The fractional light transmittance was evaluated as the photo-cell output at any time (I) divided by the photo-cell output at zero concentration (I_o).

The computer program to analyze the batch data is given in Appendix C, Computer Program 2. This program received the data set as a 9 x N array, where N is number of times each photo-cell was sampled and corresponds to the number of data cards in that set. An array in time was generated knowing the scanning rate. This array was 11 x N since there was a dummy word at the beginning and end of each data record (each card).

The initial value of fractional light transmittance was expected to be a function of the initial concentration of the slurry. By taking this initial value for each of the settling tests an attempt was made to develop the an empirical relation;

$$\frac{I}{I_o} = f(c) .$$

Figure 4.1a and 4.1b show these data as two of the photo-cells, one 30 cm from the top and the other 30 cm from the bottom. Similar plots for the other positions show identical results. It can be seen that for concentrations greater than 0.05 solids fraction the slurry was essentially opaque to the light source. Since it was necessary to study settling rates at much higher concentrations, the concentration gradients within the slurry could not be observed. These initial light transmittance values for each photo-cell are tabulated in Table B.1 (Appendix B). It is apparent that a very much stronger light source and more sophisticated detection device would be required to observe concentration gradients at higher concentrations.

The size distribution of the particles caused the slurry to settle with a very poorly defined interface. This made it impossible to visually observe the movement of the interface. Using the photo-extinction technique the settling rates were successfully determined. Figure 4.1 indicates that for a value of I/I_o greater than 0.5 the particle concentration was less than 0.005 solids fraction. Defining the slurry "interface" as the point where the concentration becomes less than 0.005, the time for the "interface" to pass each photo-cell (at 10 cm increments) was recorded. Computer Program 2 selects the first "I/I_o" value greater than 0.5 for each channel and selects the corresponding "time" value. The results are summarized in Table B.2 as the average time for the ratio I/I_o to reach a

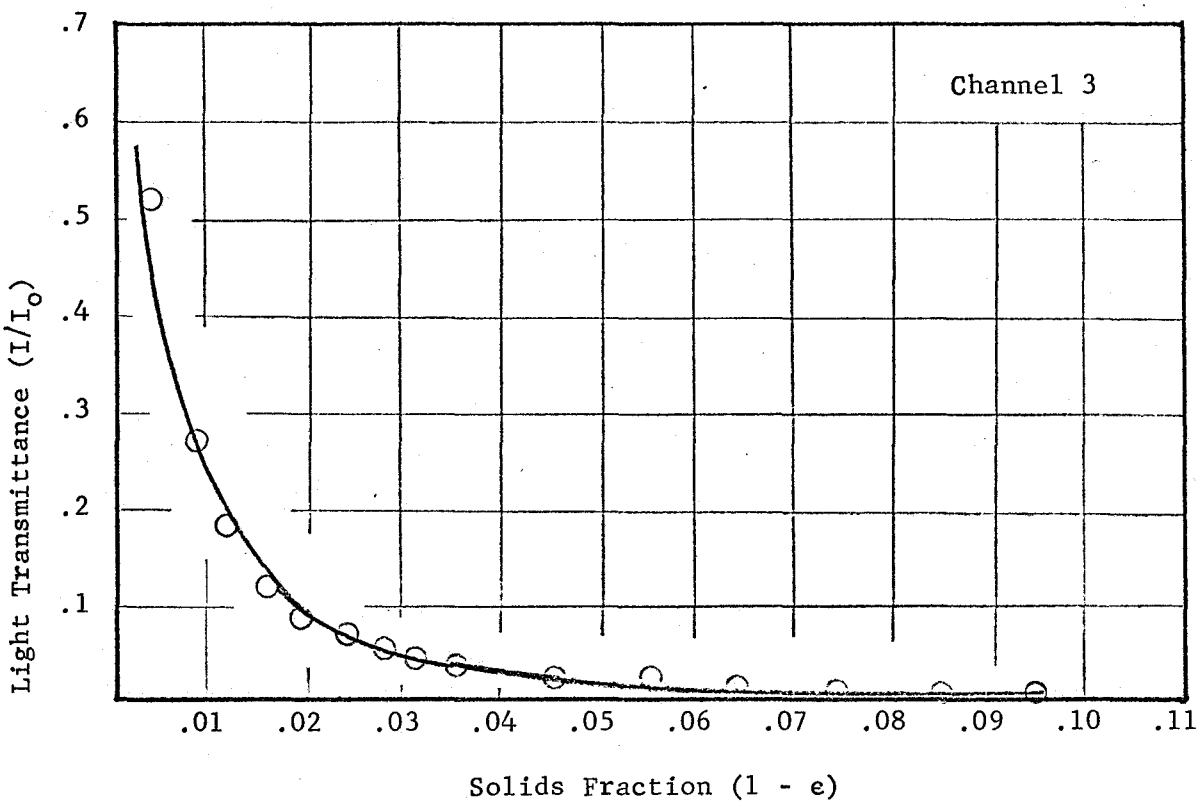

Figure 4.1a

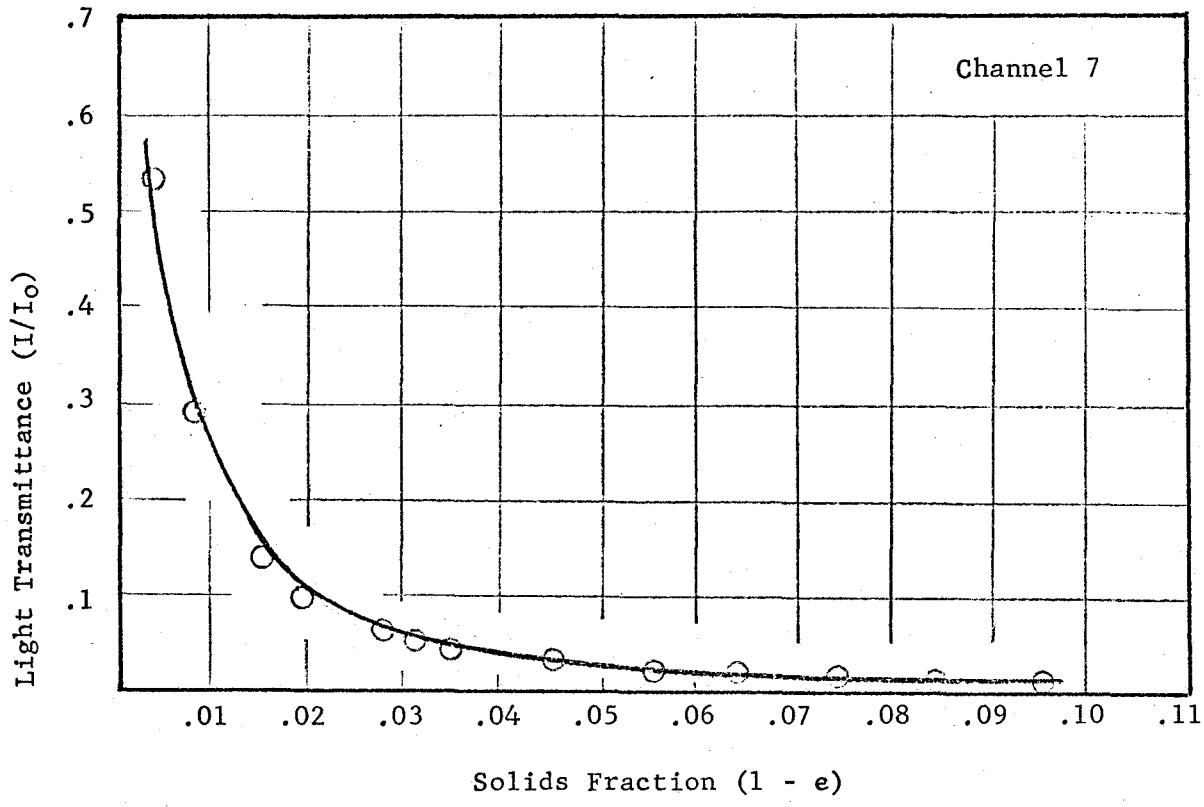

Figure 4.1b

Light Transmittance vs. Initial Solids Fraction

value greater than 0.5 for each concentration. A linear, least-squares line was passed through these points and the slope was taken to be the settling velocity.

Figure 4.2 shows several runs at different initial concentrations with the least-squares line drawn through each data set. It is interesting to note that there is no indication, for any of these tests, of a decreasing rate period. It appeared that the slurry settled at a constant rate to the ultimate (settled) concentration. The residual sums of squares of the least-squares fit indicated that the straight line approximation was valid at a 99.5% confidence level in every case. Even at the high concentrations when the settled solids blocked all but two or three of the photo-cells, the straight line still extrapolated very close to zero depth at time equal to zero. Because the photo-cells were spaced 10 cm apart the "knee" in these settling curves was not actually recorded. The ultimate depth of the mass of settled particles was noted and these are also shown in Figure 4.2.

The settling velocity, v, was evaluated at initial concentration values from 0.008 to 0.476 solids volume fraction, (1 - ϵ). The average values of the replicate runs are shown on Figure 4.3 and a smoothed curve was constructed through these points. These results and the settling velocity corrected for return flow (v/ϵ) are summarized, together with the solids flux per unit area (G) in Table B.3, Appendix B.

This curve of v vs. (1 - ϵ) should extrapolate to the Stokes' velocity, v_s, at (1 - ϵ) = 0. The Stokes' velocity for a single sphere of the material used in this study using the mean particle diameter, 285 microns, is 14.58 cm/min. The particle density used in this calculation

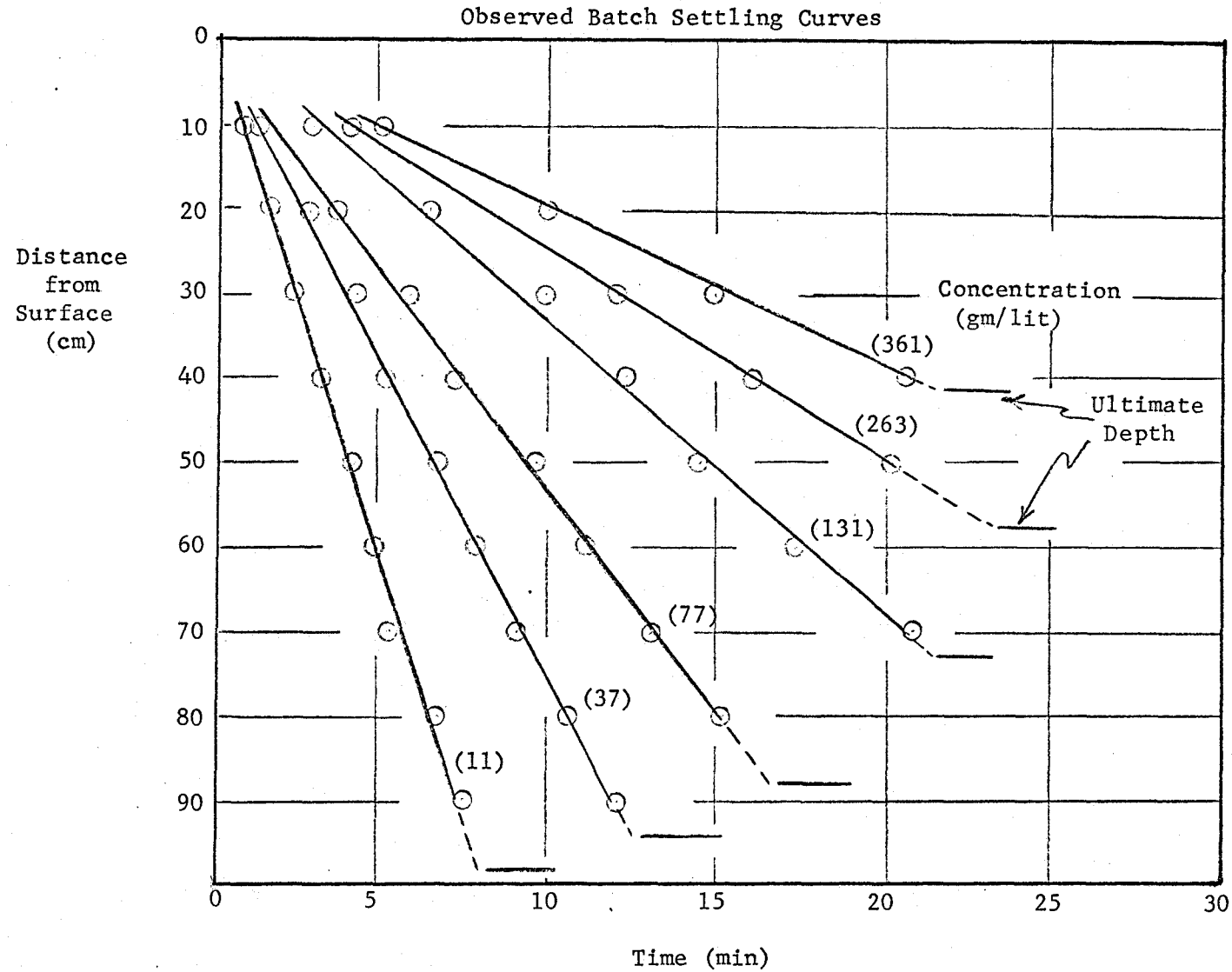

Figure 4.2

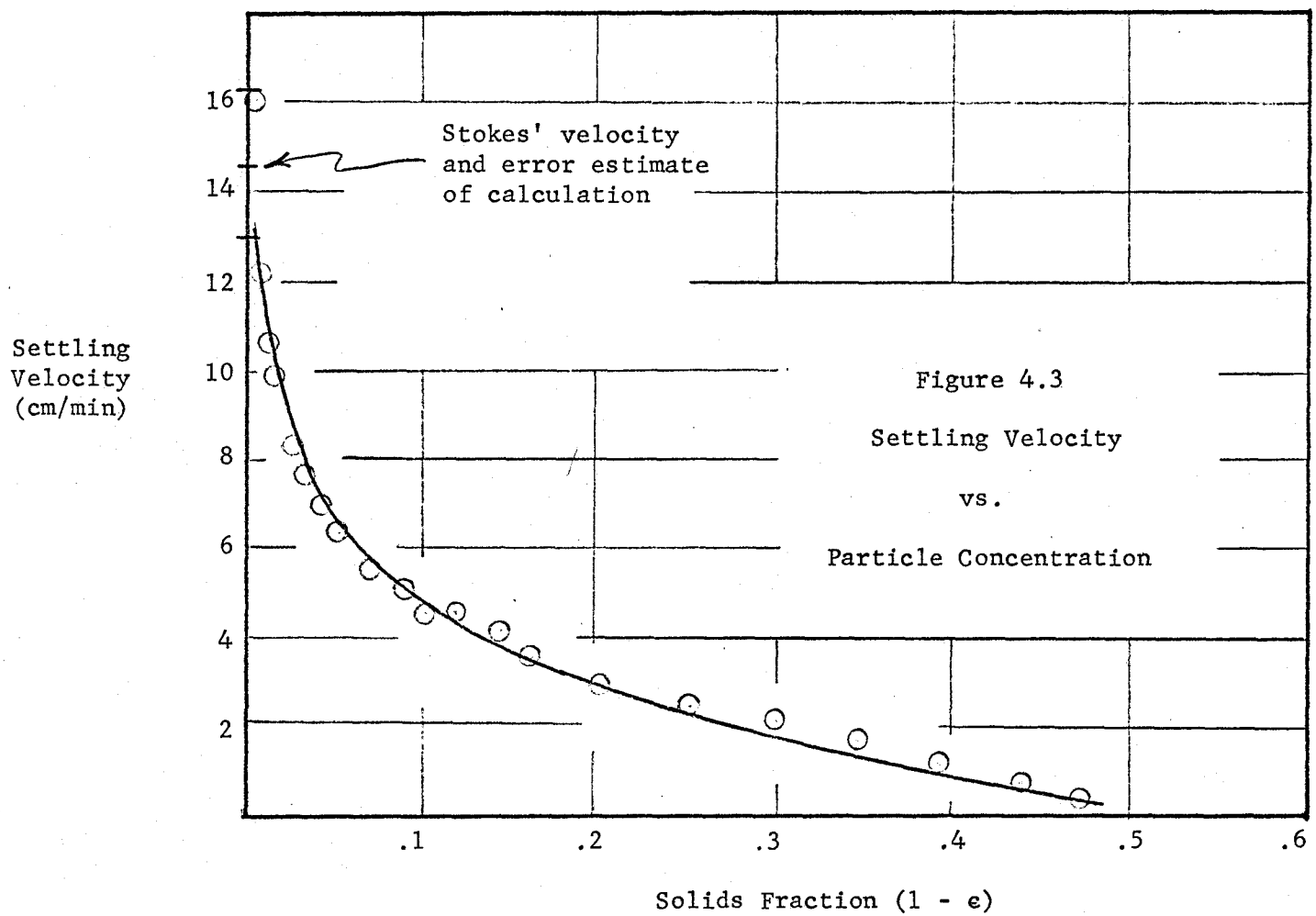

Figure 4.3

Settling Velocity

vs.

Particle Concentration

was 1.04 gm/cc with an estimated experimental error of 0.5%. This leads to an error of 10% or $\pm$ 1.65 cm/min in the Stokes' velocity. This large numerical error results from subtracting two numbers of almost equal magnitude, the solid and liquid densities. Further, the settling velocity should approach zero as the concentration nears the ultimate value. The volume fraction solids of the settled particles, the ultimate value for the particle concentration, was calculated using the final settled depth, the amount of solids in the vessel and the cross-sectional area of the vessel. A fifth order polynomial was fitted to the data and extrapolated to t = 0. The intercept value was 14.47 cm/min which compares very closely to the calculated Stokes' velocity of 14.58 cm/min. This curve did not extrapolate to a meaningful ultimate concentration but Figure 4.3 does indicate that the calculated value of $(1 - \epsilon_p) = 0.595$ is in agreement with the shape of the curve near the ultimate concentration.

The analytical relations described in Section 2.1 to evaluate the settling velocity as a function of particle concentration were compared to the experimental results of this study. The most successful was the equation given by Happel and Brenner (1965). The Happel and Brenner equation is also the one with the firmest fundamental significance since it results from a theoretical analysis. The experimental results are compared to the Happel and Brenner relation in Figure 4.4. Although the absolute value of the deviation between the experimental and the predicted settling velocities is quite small, at the higher concentrations this is quite a significant relative error.

The batch flux per unit area was evaluated for each experimental run. The averages of the replicate sets of each concentration are shown

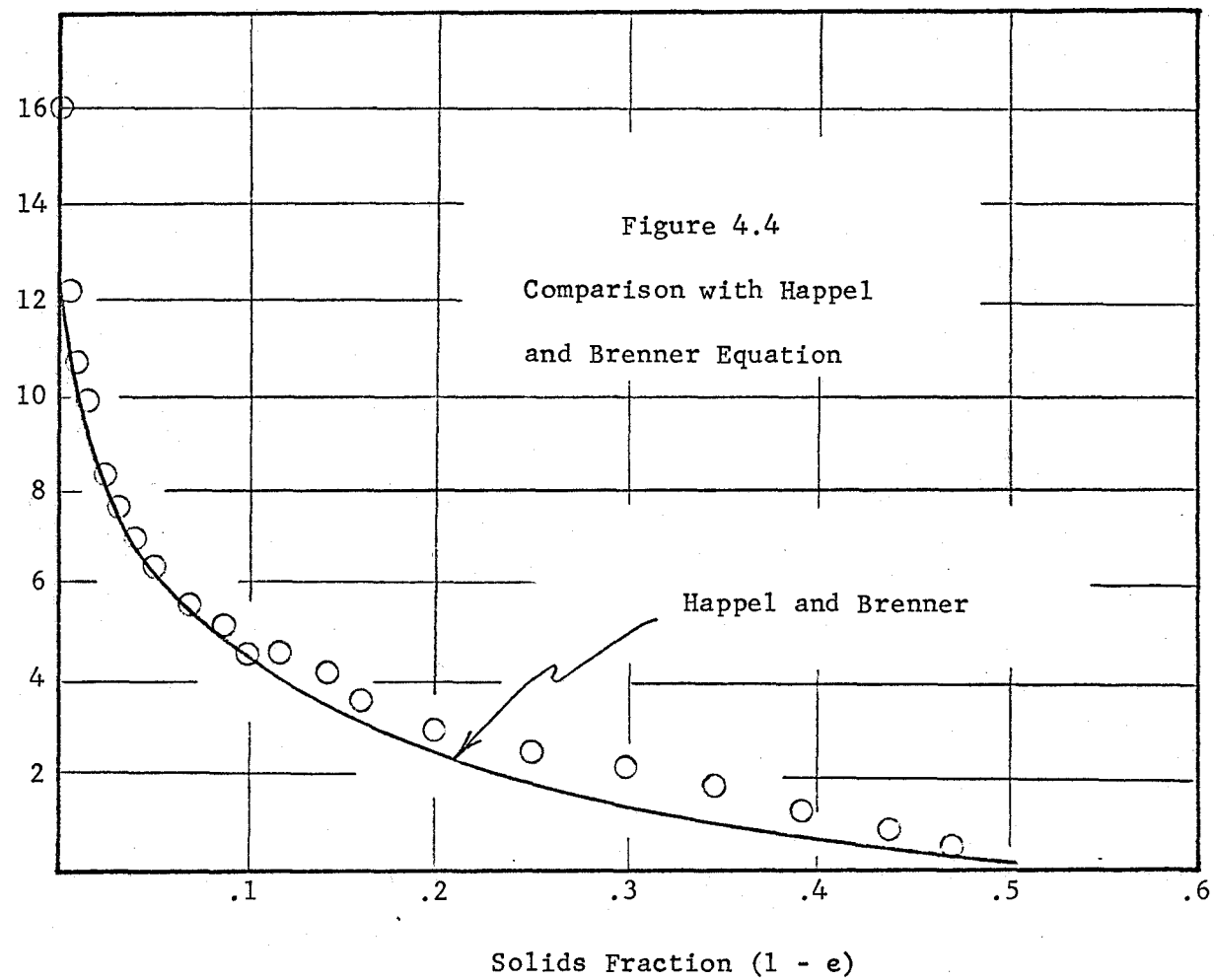
Figure 4.4
Comparison with Happel
and Brenner Equation
Settling
Velocity
(cm/min)
16
14
12
10
8
6
4
2
.1
.2
.3
.4
.5
.6
Happel and Brenner
Solids Fraction (1 - e)

Figure 4.4

on Figure 4.5 and the shape of this batch flux plot suggested. The data indicate one inflection point at approximately (1 - ϵ) = 0.48; that is, the curve becomes convex with respect to the origin beyond this concentration value. Shannon, et. al. (1963) have reported a study of batch settling rates for small (67 microns) glass spheres. These authors presented a flux plot of a very similar shape, but suggest a second inflection point to give second "concave downwards" region where the flux becomes zero at the ultimate solids concentration.

The relation between solids flux and concentration was calculated by the Happel and Brenner equation. The experimentally observed solids flux is compared to that calculated in Figure 4.6. The small absolute deviations between the observed and calculated settling velocities at the high concentrations (Figure 4.4) result in large differences when the flux is calculated by the Happel and Brenner equation. In addition, the flux does not become zero at the ultimate solids concentration.

4.2 Results from Continuous Settler Studies

Observations were made of the concentration profile within the sedimentation zone of the continuous settler during steady state operation. As with the batch studies, the light extinction technique was limited to relatively low concentrations of particles.

The raw data from the continuous unit was interpreted on the computer using Computer Program 3, Appendix C. The results of the light transmittance readings are given in Table B.4 and the material balance for each steady state operation is summarized in Table B.5, Appendix B.

The light transmittance data of two typical photo-cells (one 30 cm from the inlet feed distribution and the other 30 cm from the bottom) is

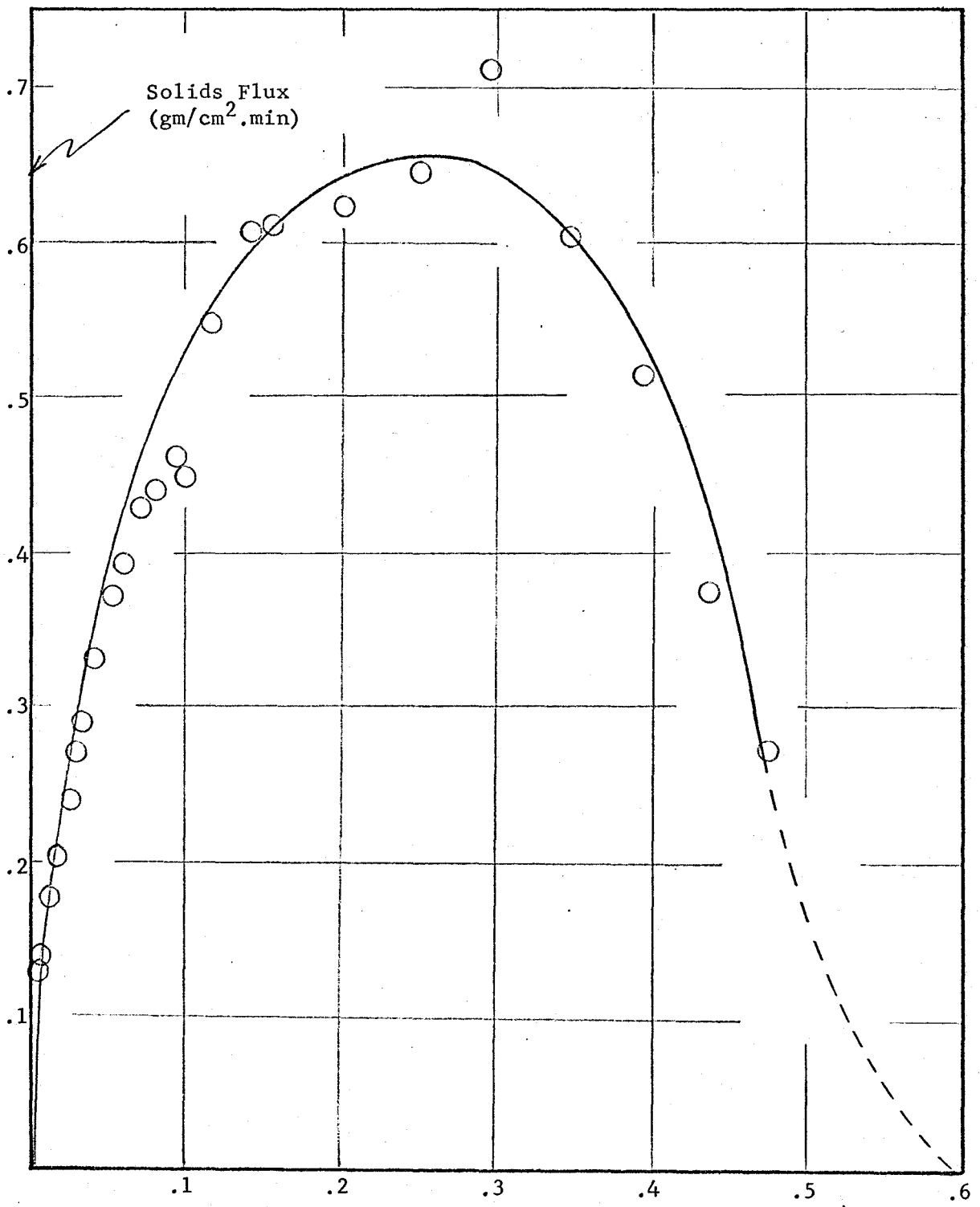

Figure 4.5

Observed Batch Flux Plot

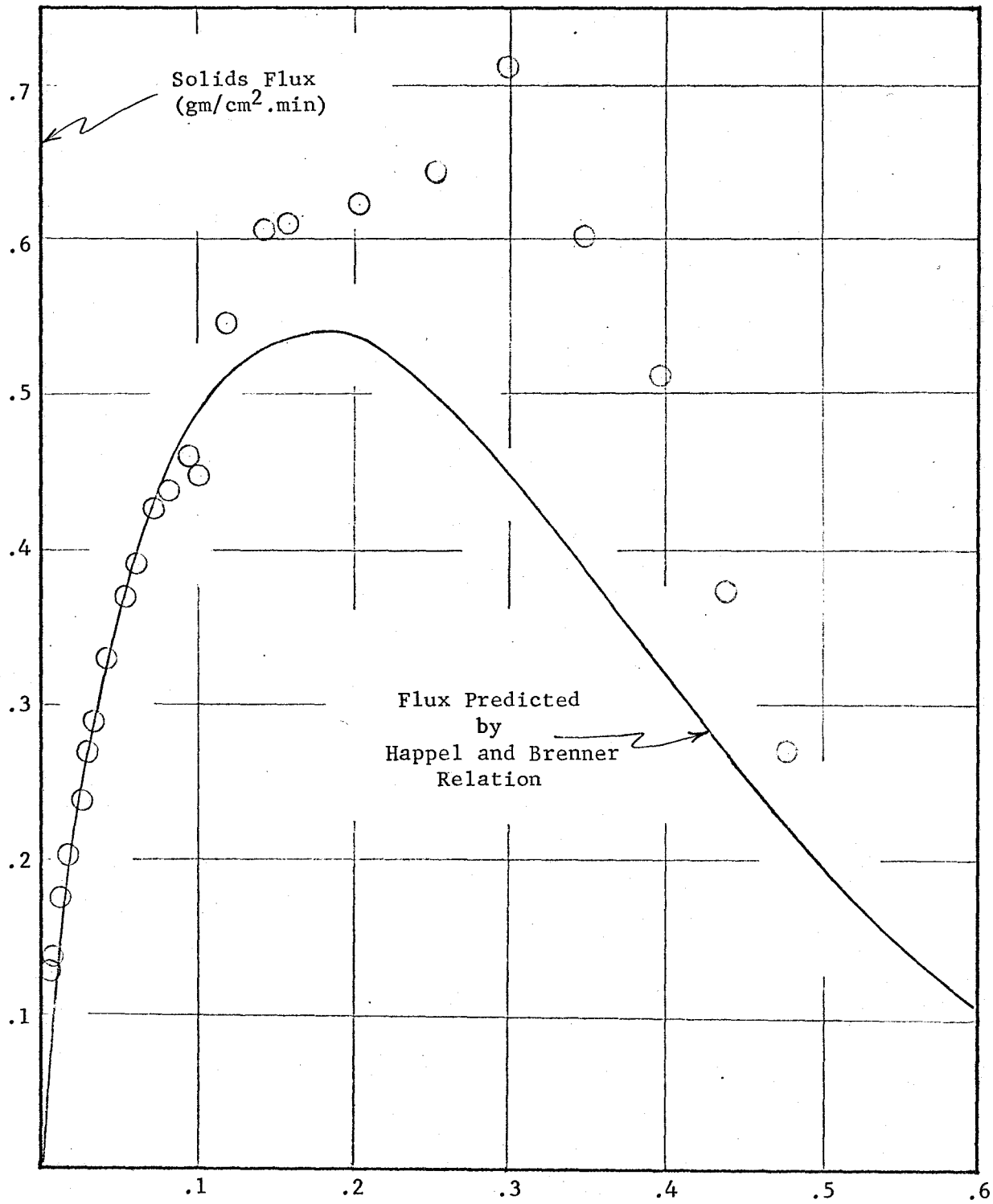

Figure 4.6

Batch Flux by Happel and Brenner Relation

plotted against the feed slurry concentration in Figures 4.7a and 4.7b. A plot of the other photo-cells gives essentially similar results.

The light transmittance results from the batch studies were used to evaluate the concentration within the sedimentation zone of the continuous unit. Figure 4.1 shows the relation between transmitted light and particle concentration assuming that the slurry was uniformly mixed at the start of the batch run. Applying this correlation to the data from the continuous unit, it was shown that the particle concentration was the same at each point within the sedimentation zone. The varying concentration profile predicted by the theory and used as the basis for design was not observed. At any steady state operation the concentration profile with depth was a constant depending on the feed rate and the concentration in this region was, in fact, less than the feed concentration. The fact that the slurry concentration in the settler was less than that of the feed could only have resulted if the particles could always settle at a greater solids flux than the rate of input of solids.

The operation of the settler was limited in each case by the clarification capacity: the solids limiting situation could not be reached. For example, an overflow of 220 ml/min gives an upward velocity of 3.7 cm/min. Using Stokes' Law a particle with a diameter of less than 144 microns would be carried out with the overflow. From the particle size distribution (Figure 3.6) this corresponds to 3% of the particles. Thus, a small part of the feed slurry was "washed out".

Section 2.2 described how batch settling tests can be used to predict the performance of a continuous settler. The Coe and Clevenger (1916) approach and the flux plot constructions all result in the same design

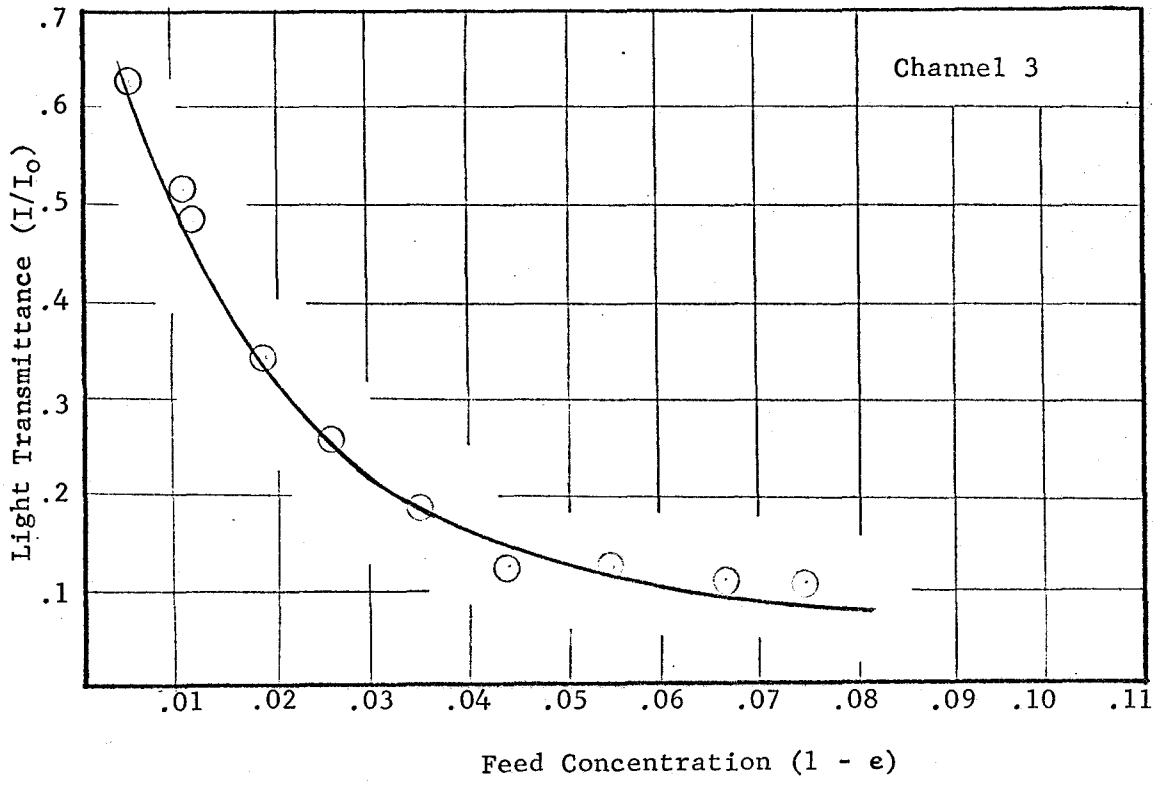

Figure 4.7a

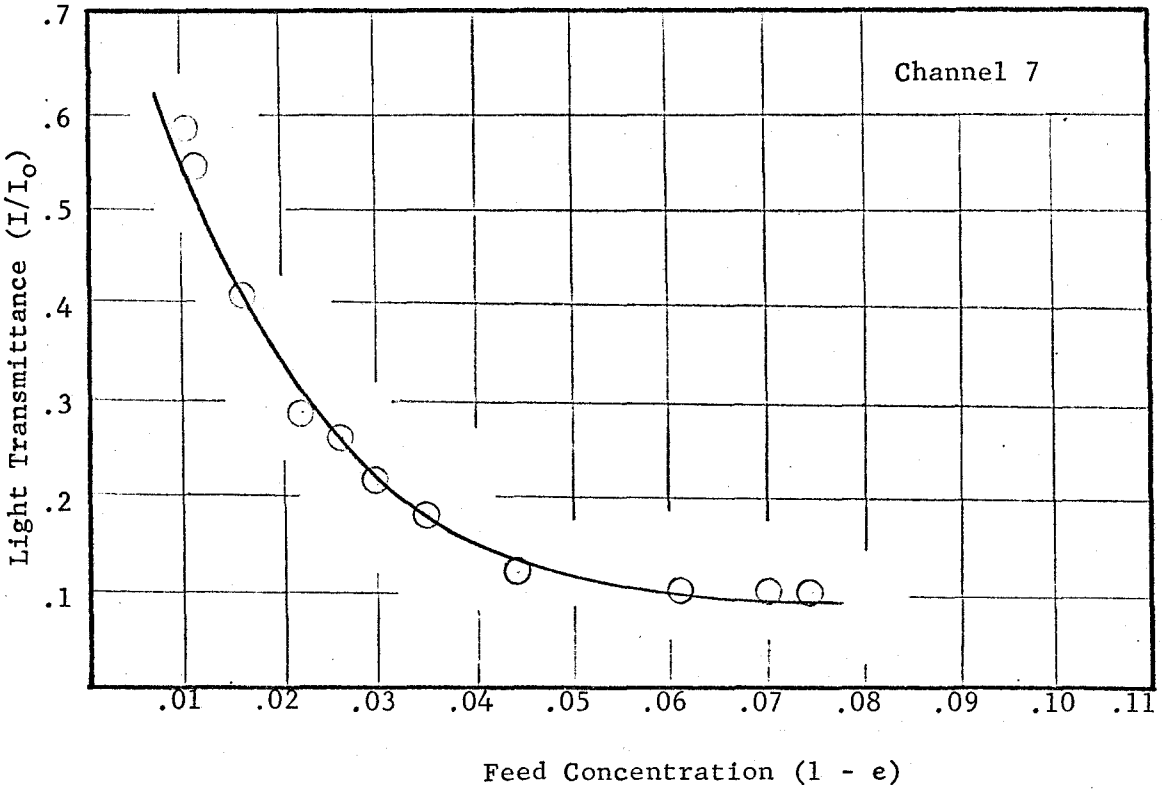

Figure 4.7b

Light Transmittance vs. Feed Concentration

equation:

$$G_{min} = \frac{v_L}{\left[\frac{1}{C_L} - \frac{1}{C_u}\right]} \qquad \ldots (15).$$

The Coe and Clevenger technique consists of plotting,

$$G_i = \frac{v_i}{\left[\frac{1}{C_i} - \frac{1}{C_u}\right]} \qquad \text{vs. } C_i \ ,$$

where; C_u is the desired underflow concentration.

The minimum flux, G_{min}, between C_f, the feed concentration, and C_u is then selected as the basis of the settler area requirement.

To illustrate this procedure an underflow concentration, C_u, of 250 gm/lit was selected and the resulting G_i vs. C_i curve is shown in Figure 4.8. For any value of feed concentration the minimum flux, G_{min}, will occur at that feed concentration. For example, if a feed concentration of 75 gm/lit is chosen, then G_{min} = 0.6 gm/cm^2 min.

Also shown in Figure 4.8 is the batch flux plot. This curve can also be used to determine G_{min} by drawing a straight line from C_u, through C_f to intersect the ordinate at G_{min}. It can be seen that the two techniques give the same result.

This graphical construction is a very convenient method to determine the limiting solids flux for any desired underflow concentration. It has been shown (Section 2.2) that if this "operating line" intersects the flux curve anywhere between C_f and C_u the solids will accumulate in the sedimentation zone and eventually overflow. For any reasonable choice of C_f and C_u on Figure 4.8 this condition would not be violated. In fact, this solids limiting condition will develop only when the flux plot exhibits a very pronounced convex section at concentrations below the

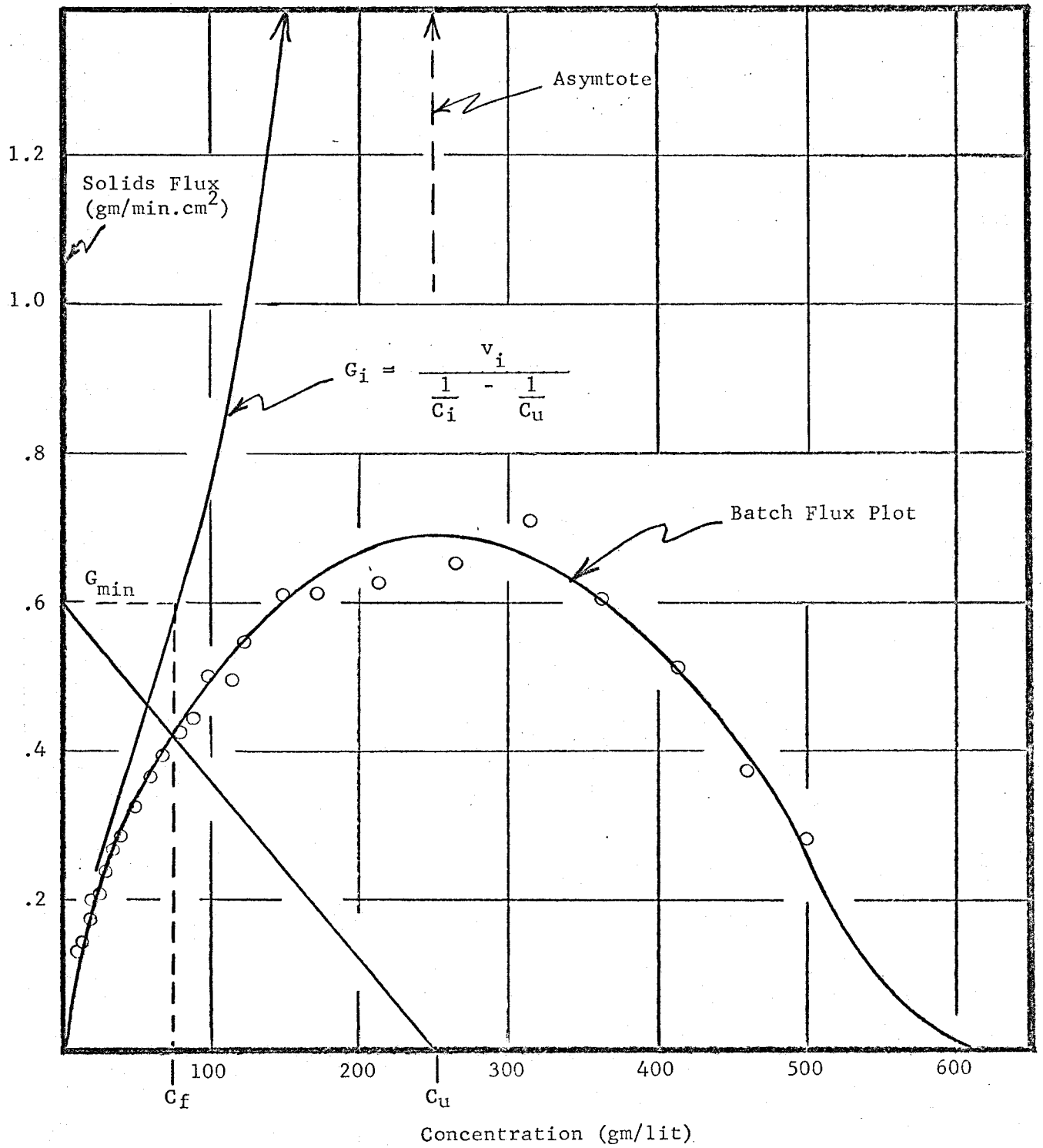

Figure 4.8

Flux Plot Construction

desired underflow value (Figure 2.8 has illustrated this condition).

This discussion has shown that for any material which gives a batch flux plot that is essentially a single concave downwards plot the continuous settler will always be limited by the clarification capacity, i.e. the upflow velocity.

The flow rates and concentrations at each steady state operation of the continuous settling apparatus are summarized in Table B.5. The liquid balance,

$$Q_u + Q_e = Q_f \ ,$$

has a closure of less than 4%. The solids balance,

$$G_u = G_f \ ,$$

closes to within 5% in most cases. This precision was not great enough to detect the weight fraction carried out with the overflow, but it does suggest that the steady state assumption is valid.

At the lower concentrations it is possible to use the light intensity readings from the steady state operation of the continuous unit to determine the particle concentration in the sedimentation zone. The light transmittance vs. initial concentration from the batch studies can be used for this purpose. The settling velocity of the particles in the continuous unit can then be calculated by:

$$G = C \ (v + V)$$

The value of "G" was measured and "V" was calculated knowing the underflow rate and the cross-sectional area. The settling velocity, v, calculated in this manner was then compared to the batch settling velocity at that concentration. This comparison is shown in Figure 4.9. Since the higher concentrations were opaque to the light source, the corresponding settling velocities could not be compared in this way. This correla-

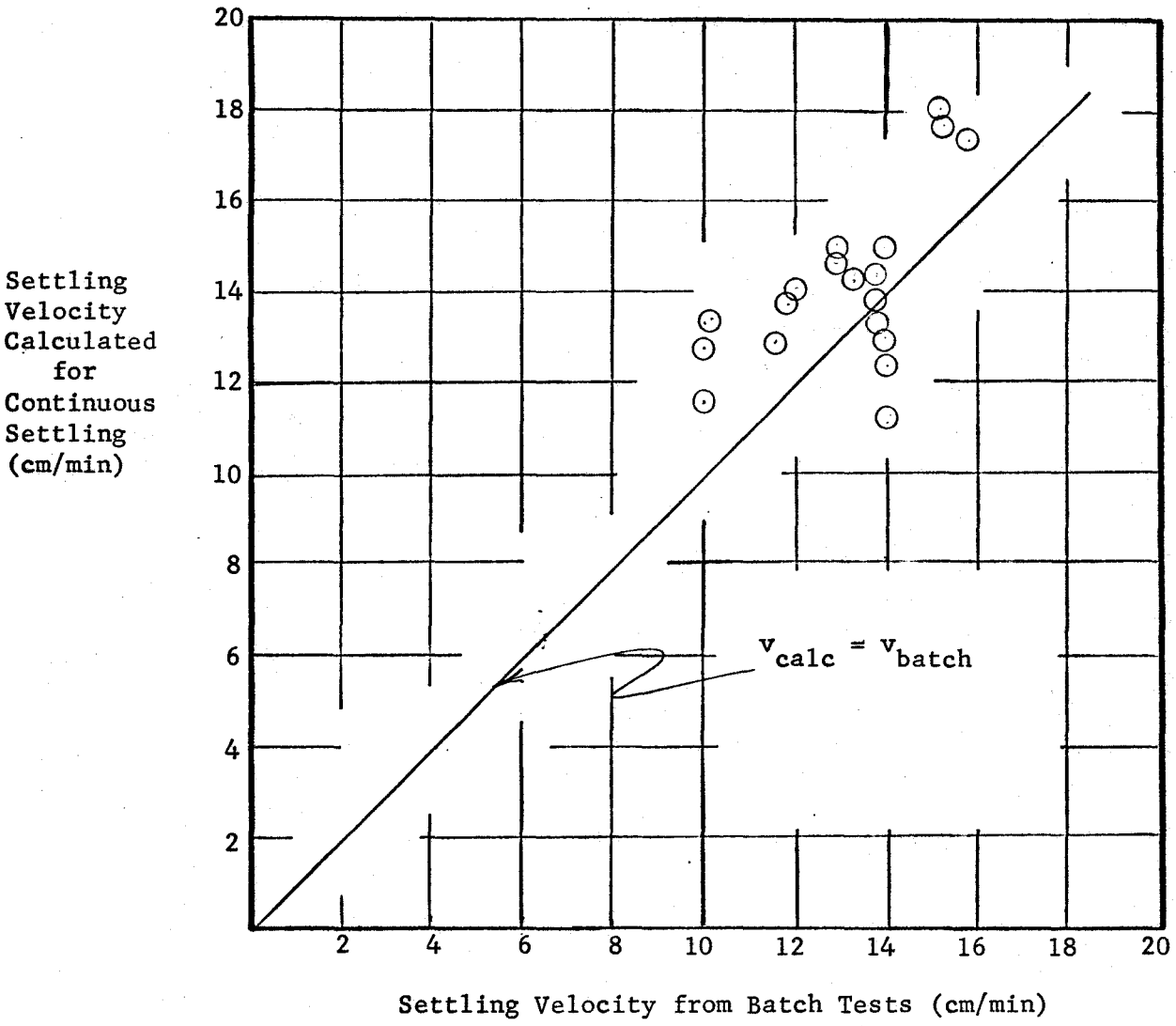

Figure 4.9

Comparison of Batch and Continuous Settling Velocities

tion shows that the settling velocity in batch tests are related to the particle settling velocity in a continuous unit.

The maximum overflow rate that would just carry out a small fraction of the particle was selected. This could be controlled by observing the number of particles rising in the clarification zone. Operating in this manner the solids limitation of the vessel was never exceeded. The light transmittance data suggested a uniform concentration profile throughout the sedimentation zone and the solids flux per unit area was less than the value of G_{min} determined by the batch flux plot. For example, the feed concentration of one run was 78.2 gm/lit and the underflow concentration was 213 gm/lit. On the batch flux plot the corresponding value of G_{min} is 0.65 gm/cm^2 min. The experimentally determined solids flux was:

$$\frac{23.38 \text{ gm/min}}{61.9 \text{ cm}^2} = 0.38 \text{ gm/cm}^2 \text{ min}$$

Any attempt to reach a solids limiting condition would increase the flow rate and thus exceed the clarification capacity of the vessel.

CHAPTER 5

SUMMARY AND CONCLUSIONS

(1) The photo-extinction technique can be used to observe batch settling rates. To detect concentration profiles within a concentrated slurry a more sophisticated light source and detection device would be required. The apparatus used in this study was quite successful in determining the settling rate of a slurry settling with a poorly defined interface.

(2) The particles used in this study were discrete spheres and settled at a constant rate to an incompressible bed. No decreasing rate, or compression, phase could be detected at any initial concentration.

(3) At particle concentrations approaching the ultimate concentrations, packed bed, the batch flux plot exhibits an inflection point and becomes convex downward. However, the curvature in this region is so small that the flux plot is essentially concave everywhere.

(4) The shape of the batch flux plot predicts that the limitations in continuous settler operation will always be the upward overflow velocity in the clarification zone.

(5) The operation of the continuous settling apparatus agreed with these predictions. The solids flux limitation of the vessel could not be exceeded without greatly exceeding the clarification capacity. Light transmittance data for the continuous unit suggested a uniform concentration profile in the sedimentation zone.

(6) The concentration of particles within the sedimentation zone of the continuous settler was less than the feed concentration.

(7) The conventional design procedure that selects the required area of a continuous settler based only on solids flux limitation will result in serious under-design for a material with settling characteristics similar to that observed in this work. The performance of a continuous unit with this type of material will always be governed by the clarification capacity.

(8) The settling velocities observed in batch settling tests can be compared to the particle settling velocities at the same concentration in a continuous unit.

REFERENCES

1. Brinkman, H.C.
   A Calculation of the Viscous Force Exerted by a Flowing Fluid on a Dense Swarm of Particles
   Appl. Sci. Res., A1, 27 (1947)

2. Coe, H.S. and Clevenger, G.H.
   Methods of Determining the Capacity of Slime-Settling Tanks
   Trans. Amer. Inst. Mining Eng., 55, 356 (1916)

3. Cole, R.F.
   Experimental Evaluation of the Kynch Theory
   Ph.D Thesis, U. of N. Carolina (1968)

4. Comings, E.W.
   Thickening of Calcium Carbonate Slurries
   I & EC, 32, 663 (1940)

5. _____ ; Pruiss, C.E. and Debord, C.
   Continuous Settling and Thickening
   I & EC (Indust.), 46, 1164 (1954)

6. Fuerstenau, M.C.
   The Mechanism of Thickening Kaolin Slurries
   D.Sc. Thesis, MIT (1960)

7. Happel, J.
   Viscous Flow in Multiparticle Systems
   AIChE J., 4, 197 (1958)

8. _____ ; and Brenner, H.
   Low Reynolds Number Hydrodynamics
   Prentice-Hall Inc., Englewood Cliffs, N.Y. (1965)

9. Kynch, C.J.
   A Theory of Sedimentation
   Trans. Far. Soc., 48, 166 (1952)

10. Oliver, D.R.
    The Sedimentation of Closely-Sized Spherical Particles
    Chem. Eng. Sci., 15, 230 (1961)

11. Richardson, J.F. and Zaki, W.N.
    Sedimentation and Fluidization: Parts 1-4
    Trans. Inst. Chem. Engrs., 32, 35 (1954): 36, 270 (1958): 39, 348 (1961): 39, 357 (1961)

12. Roberts, E.J.
    Thickening - Art or Science?
    Trans. AIME, 184, 61 (1949)

13. Robins, W.H.M.
The Theory of Design and Operation of Settling Tanks
Trans. Instn. Chem. Eng., 42, T158 (1964)

14. Scott, K.J.
Thickening of Calcium Carbonate Slurries - Comparison of Data with Rigid Spheres
I & EC (Fundamentals), 7, 3, 484 (1968a)

15. _____ ;
Experimental Study of Continuous Thickening of a Flocculated Silica Slurry
I & EC (Fundamentals), 7, 4, 582 (1968b)

16. Shannon, P.T.; Stroupe, E. and Tory, E.M.
Batch and Continuous Thickening
I & EC (Fundamentals), 2, 3, 203 (1963)

17. _____ ; and Tory, E.M.
Settling of Slurries
I & EC, 57, 18 (1965)

18. Steinour, H.H.
Rate of Sedimentation
I & EC, 36, 7, 619 (1944)
36, 7, 840 (1944)
36, 7, 901 (1944)

19. Talmage, W.P. and Fitch, E.B.
Determining Thickener Unit Areas
I & EC, 47, 1, 38 (1955)

20. Tory, E.M.
Batch and Continuous Thickening of Slurries
Ph.D Thesis, Purdue Univ., Ind. (1961)

21. Vand, V.
Viscosity of Solutions and Suspensions
J. Phys. & Colloid Chem., 52, 277 (1948)

APPENDIX A

Nomenclature

A	=	cross-sectional area
C	=	concentration of particle
D_p	=	mean particle diameter
g	=	gravitational force
G	=	solids flux
I	=	light intensity
N_{Re}	=	Reynolds Number
Q	=	volumetric flow rate
f	=	time
u	=	velocity of concentration discontinuity
v	=	settling velocity
v_s	=	Stokes' Law velocity
v_H	=	hindered settling velocity
V	=	velocity component resulting from underflow rate
z	=	depth
ϵ	=	void fraction
$1 - \epsilon$	=	solids fraction
ρ	=	density of liquid
ρ_s	=	density of solids
μ	=	viscosity of liquid

APPENDIX A (Continued)

Subscripts

e	=	overflow
f	=	feed
L	=	limiting
min	=	minimum; lowest value of solids handling capacity (flux) between feed and underflow of continuous unit
o	=	initial; t = 0
p	=	ultimate on "packed bed" value
u	=	underflow

APPENDIX B

TABLE B.1

Initial Light Transmittance at Each Position

Concentration (1 - e)	(Top) Photo-Cell Number 1	2	3	4	5	6	7	8	(Bottom) 9
.004	0.62	0.59	0.52	0.56	0.49	0.55	0.54	0.50	0.51
.008	.34	.31	.27	.30	.26	.30	.29	.27	.29
.011	.24	.22	.19	.22	.18	.23	.22	.19	.21
.015	.16	.14	.12	.15	.12	.15	.14	.12	.14
.019	.12	.10	.09	.11	.09	.11	.10	.09	.10
.024	.10	.09	.08	.10	.07	.10	.09	.08	.10
.027	.08	.07	.06	.08	.06	.08	.07	.06	.07
.031	.07	.06	.05	.06	.05	.06	.06	.04	.06
.035	.06	.05	.04	.05	.04	.05	.05	.04	.05
.045	.05	.04	.03	.04	.03	.04	.03	.03	.03
.055	.04	.03	.03	.03	.02	.03	.03	.02	.03
.064	.04	.03	.02	.03	.02	.03	.02	.02	.03
.074	.03	.02	.02	.02	.02	.02	.02	.02	.02
.084	.03	.02	.02	.02	.02	.02	.02	.02	.02
.095	.02	.02	.01	.02	.01	.02	.02	.01	.02
.105	.02	.02	.01	.02	.01	.02	.02	.01	.02
.118	.02	.02	.01	.02	.01	.02	.02	.01	.02
.143	.02	.01	.01	.01	.01	.01	.01	.01	.01
.164	.02	.01	.01	.01	.01	.01	.01	.01	.01

TABLE B.2

Time Required for Light Transmittance to Reach 0.5

Concentration (1 - e)	(Top) Photo-Cell Number, Time (Min) (Bottom)								
	1	2	3	4	5	6	7	8	9
.008	0.53	1.32	1.85	2.38	3.16	3.70	4.23	5.27	5.80
.011	0.79	1.57	2.36	3.14	4.18	4.59	5.37	6.54	7.32
.015	0.95	1.82	2.85	3.63	4.92	5.45	6.32	7.52	8.39
.019	1.03	2.07	3.11	3.98	5.18	5.96	6.80	8.28	9.06
.024	1.03	2.32	3.67	4.71	6.09	6.97	8.26	9.55	10.64
.027	1.29	2.45	3.86	4.90	6.31	7.22	8.39	9.80	10.83
.031	1.29	2.58	3.95	4.98	6.44	7.30	8.59	10.05	11.00
.035	1.20	2.64	4.03	5.07	6.69	7.56	8.93	10.39	11.59
.045	1.31	3.04	4.68	5.99	7.51	8.50	10.13	11.76	13.07
.055	1.50	3.23	4.95	6.13	8.06	9.29	10.77	12.68	14.05
.064	1.54	3.37	5.19	6.50	8.55	9.83	11.64	13.88	
.074	1.68	3.78	5.73	7.14	9.38	10.65	12.60	14.70	
.084	1.67	3.87	5.96	7.63	9.84	11.53	13.46	15.21	
.095	2.08	4.16	6.37	7.90	10.12	12.06	13.73	16.07	
.105	2.08	4.70	7.05	8.86	11.36	13.28	15.63	17.98	
.118	2.48	5.12	7.60	9.60	11.92	13.75	16.23		
.143	2.52	5.80	8.51	10.46	13.08	14.94	17.84		
.164	2.90	6.36	9.54	11.85	14.48	17.09	20.27		
.203	3.42	6.83	10.54	13.67	17.37	20.22			
.252	4.02	8.34	12.36	16.39	20.41				
.299	4.82	9.36	13.34	18.16					
.346	5.27	10.55	16.55	23.85					
.394	7.20	13.85	22.42						
.438	9.38	21.59							
.476	12.20	30.63							

TABLE B.3

Calculated Settling Rate and Flux for Batch Tests

Concentration C (gm/lit)	(1 - ε) -	Settling Velocity v (cm/min)	Solids Flux G (cm/sq.cm * min)	Corrected for Return Flow Settling Velocity v/e (cm/min)	Solids Flux G/e (gm/sq.cm * min)
8.04	.008	16.16	.1299	16.28	.1310
11.10	.011	12.37	.1372	12.50	.1387
16.08	.015	10.79	.1735	10.96	.1762
20.08	.019	9.98	.2002	10.17	.2041
24.73	.024	8.39	.2074	8.59	.2124
28.26	.027	8.36	.2363	8.58	.2432
32.56	.031	8.23	.2680	8.50	.2767
36.94	.035	7.79	.2878	8.08	.2983
47.33	.045	6.93	.3280	7.26	.3429
56.90	.055	6.44	.3665	6.81	.3877
66.99	.064	5.85	.3920	6.25	.4189
77.07	.074	5.52	.4258	5.97	.4604
87.65	.084	4.99	.4369	5.44	.4669
99.34	.095	5.09	.5054	5.63	.5589
110.00	.105	4.49	.4938	5.02	.5520
122.85	.118	4.47	.5487	5.06	.6218
148.93	.143	4.08	.6076	4.76	.7087
171.07	.164	3.57	.6105	4.27	.7302
211.78	.203	2.95	.6243	3.70	.7833
263.12	.252	2.45	.6448	3.28	.8620
312.25	.299	2.28	.7101	3.25	1.0131
361.18	.346	1.67	.6028	2.55	.9216
411.39	.394	1.25	.5135	2.06	.8441
457.33	.438	.82	.3748	1.45	.6670
497.45	.476	.54	.2700	1.03	.5158

TABLE B.4

Light Transmittance Readings in Continuous Settler

Feed Concentration (gm/lit)	(1 - ε)	Photo-Cell 1	2	3	4	5	6	7	8	9
5.71	.005	0.64	0.63	0.63	0.66	0.62	0.67	0.66	0.67	0.65
10.81	.010	.56	.53	.55	.60	.54	.58	.58	.59	.57
9.97	.010	.54	.54	.56	.59	.54	.59	.58	.58	.57
11.23	.011	.50	.49	.50	.56	.50	.55	.55	.56	.54
11.37	.011	.51	.51	.51	.55	.52	.55	.53	.54	.52
11.56	.011	.52	.51	.52	.56	.50	.55	.54	.54	.51
11.87	.011	.52	.50	.51	.55	.50	.54	.52	.54	.52
12.65	.012	.50	.47	.48	.52	.46	.50	.50	.52	.50
12.12	.012	.49	.47	.48	.53	.49	.51	.51	.52	.50
13.76	.013	.46	.46	.48	.53	.47	.50	.51	.52	.51
14.03	.013	.46	.45	.47	.51	.46	.49	.51	.51	.51
16.10	.015	.47	.46	.47	.51	.46	.49	.49	.50	.48
16.40	.016	.47	.45	.47	.50	.47	.51	.51	.51	.49
16.09	.015	.41	.40	.41	.46	.42	.45	.45	.45	.43
16.57	.016	.38	.38	.39	.43	.37	.41	.40	.41	.39
16.67	.016	.37	.37	.38	.42	.37	.40	.40	.41	.40
17.41	.017	.37	.37	.37	.40	.35	.39	.39	.40	.38
17.33	.017	.37	.36	.37	.42	.37	.40	.39	.40	.38
20.22	.019	.33	.33	.34	.39	.33	.37	.35	.36	.34
23.57	.023	.27	.25	.27	.31	.27	.30	.29	.30	.29
23.34	.022	.27	.26	.28	.32	.26	.30	.29	.31	.29
23.75	.023	.27	.27	.28	.32	.26	.29	.28	.30	.29
26.65	.026	.24	.23	.25	.28	.24	.27	.26	.27	.26
26.59	.026	.24	.24	.25	.28	.23	.26	.26	.28	.26
27.42	.026	.25	.24	.25	.28	.24	.27	.26	.27	.25
28.57	.027	.24	.23	.24	.27	.21	.25	.24	.25	.24
28.43	.027	.21	.20	.21	.25	.20	.23	.22	.23	.21
31.13	.030	.20	.20	.20	.24	.19	.21	.20	.21	.20
31.52	.030	.21	.21	.22	.25	.20	.23	.22	.23	.22
31.85	.031	.21	.21	.22	.25	.20	.23	.22	.23	.21
32.88	.032	.19	.18	.19	.22	.18	.21	.19	.20	.19
34.92	.034	.19	.19	.19	.22	.18	.21	.20	.21	.20
37.77	.036	.18	.17	.18	.21	.16	.19	.18	.19	.18
36.53	.035	.18	.17	.18	.21	.17	.19	.18	.19	.18
40.82	.039	.16	.15	.16	.19	.15	.16	.17	.17	.16
45.42	.044	.12	.11	.12	.14	.11	.13	.12	.13	.12
48.68	.047	.10	.11	.11	.14	.10	.12	.11	.12	.12
57.61	.055	.11	.11	.12	.14	.11	.12	.12	.13	.12
51.19	.050	.12	.11	.12	.14	.11	.13	.12	.13	.12
54.40	.052	.11	.11	.11	.13	.10	.12	.12	.13	.12
56.85	.055	.11	.11	.11	.13	.10	.12	.11	.12	.12

TABLE B.4 (Continued)

Feed Concentration (gm/lit)	(1 - e)	Photo-Cell 1	2	3	4	5	6	7	8	9
63.12	.061	.10	.10	.11	.12	.09	.11	.10	.11	.11
68.76	.066	.10	.10	.10	.11	.09	.10	.10	.11	.10
67.43	.066	.10	.10	.10	.11	.09	.10	.10	.10	.10
69.06	.066	.10	.10	.10	.11	.09	.10	.10	.10	.10
69.76	.067	.10	.10	.10	.11	.09	.10	.10	.10	.10
73.96	.071	.09	.09	.09	.10	.08	.09	.09	.10	.09
71.94	.069	.09	.09	.09	.11	.08	.10	.09	.10	.09
72.03	.069	.09	.09	.09	.10	.08	.10	.09	.10	.09
75.89	.073	.09	.09	.09	.10	.08	.10	.09	.10	.09
78.16	.075	.09	.09	.09	.10	.08	.10	.09	.10	.09

TABLE B.5

RESULTS FROM CONTINUOUS SETTLER

FLOW (ML/MIN)			CONCENTRATION (GM/LIT)		FLUX (GM/MIN)	
FEED	UNDERFLOW	OVERFLOW	FEED	UNDERFLOW	FEED	UNDERFLOW
446	105	340	5.7	23.2	2.54	2.44
372	99	274	10.2	38.3	3.79	3.79
370	101	274	10.0	36.9	3.69	3.73
360	100	264	11.2	39.8	4.04	3.98
360	102	268	11.4	41.4	4.09	4.22
360	100	260	11.6	41.5	4.16	4.15
353	100	260	11.9	41.6	4.19	4.16
352	96	264	12.6	46.0	4.45	4.41
360	100	260	12.1	46.5	4.36	4.65
300	98	200	13.8	42.7	4.13	4.19
292	101	198	14.0	41.1	4.10	4.16
280	98	184	16.1	46.1	4.51	4.51
280	98	184	16.4	48.7	4.59	4.77
328	100	226	16.1	54.4	5.28	5.44
352	98	256	16.6	59.1	5.83	5.79
352	98	256	16.7	59.8	5.87	5.86
353	99	256	17.4	62.9	6.15	6.23
350	98	258	17.3	61.2	6.07	6.00
354	98	256	20.2	72.9	7.16	7.14
358	102	250	23.6	82.2	8.44	8.39
366	103	264	23.3	83.0	8.54	8.55
364	104	285	23.7	82.4	8.64	8.57
362	103	262	26.7	95.1	9.65	9.80
362	104	260	26.6	93.3	9.62	9.70
356	98	257	27.4	100.2	9.76	9.82
352	98	252	28.6	100.6	10.06	9.86
350	100	252	28.4	101.4	9.95	10.14
354	99	256	30.7	111.1	10.85	10.99
344	99	244	31.1	118.3	10.71	11.71
344	98	244	31.5	113.5	10.84	11.12
342	99	250	31.8	109.3	10.89	10.82
348	102	244	32.9	117.8	11.44	12.02
350	104	248	34.9	114.0	12.22	11.86
348	104	244	37.8	119.5	13.14	12.43
348	104	248	36.5	123.1	12.71	12.81
348	104	242	40.8	125.1	14.21	13.02
348	98	250	45.4	157.1	15.81	15.40
344	102	242	48.7	166.5	16.75	16.99
328	102	220	57.6	160.2	18.90	16.34
312	104	196	51.2	147.7	15.97	15.36
340	108	240	54.4	172.5	18.50	18.62
332	104	228	56.9	179.1	18.87	18.63
332	108	236	63.1	190.4	20.96	20.57
320	104	220	68.8	216.6	22.00	22.53
320	108	224	67.4	204.6	21.58	22.09
320	108	224	69.1	200.4	22.10	21.65
320	108	224	69.8	203.4	22.32	21.97
328	110	224	74.0	209.1	24.26	23.00
328	108	224	71.9	209.3	23.60	22.61
328	112	224	72.0	206.2	23.63	23.09
316	108	212	75.9	205.6	23.98	22.21
304	108	208	78.2	213.1	23.76	23.01

APPENDIX C

COMPUTER PROGRAMS

PROGRAM NUMBER 1

```
      READ TAPE AND DECODE DATA TO LINE PRINTER AND PUNCH
      PROGRAM TST(INPUT,OUTPUT,PUNCH,TAPE5=INPUT,TAPE6=OUTPUT,TAPE7=PUNC
     1H,TAPE1)
      DIMENSION LOC(25), DATA(25)
      N = 1
      READ(5,25) M
   14 BUFFER IN(1,0) (LOC(1), LOC(25))
   10 CALL XRCL
      IF(UNIT,1) 16,11,12,16
   11 DECODE(130,20,LOC(I))  (DATA(I),I = 1,11)
      WRITE(6,21)       (DATA(I),I = 1,11)
      WRITE(7,27)       (DATA(I),I = 2,11)
      GO TO 14
   12 WRITE(6,22) N
      N = N + 1
      IF(N.GT.M) GO TO 13
      GO TO 14
   16 WRITE(6,26)
      GO TO 12
   13 STOP
   20 FORMAT( 11(4X,A5,2X) )
   21 FORMAT( 11A6 )
   22 FORMAT( 5X, 23H END OF FILE READ AFTER, I5, 8H RECORDS//)
   25 FORMAT( I5 )
   26 FORMAT( 5X, 10H ERROR      )
   27 FORMAT( 11A6 )
      END
1        6400 END OF RECORD
      M = NUMBER OF RECORDS TO BE READ
1           END OF FILE
```

PROGRAM NUMBER 2

```
      REDUCTION OF BATCH DATA
      PROGRAM TST (INPUT,OUTPUT,TAPE5=INPUT,TAPE6=OUTPUT)
      DIMENSION DATA(9,200), TIME(11,200), AVG(9,200), TI(150), M(10),
     1 DATAI(9,150), MIN(200), TOP(10), NDIST(10)
   17 READ(5,20) NRUN
      READ(5,23) SCAN, GRAM
      J = 1
   19 READ(5,21)  (DATA(I,J), I = 1,9)
      IF( DATA(1,J).EQ.100. ) GO TO 18
      J = J + 1
      GO TO 19
   18 NUM = J - 1
      N = NUM
      DO 11 J = 1,N
      DO 11 I = 1,9
      DATA(I,J) = DATA(I,J)/DATA(I,N)
   11 CONTINUE
      RATE = SCAN/100.0
      T = 1.0
      N = NUM + 2
      DO 12 J = 1,N
      DO 12 I = 1,11
      TIME(I,J) = RATE*T
      T = T + 1.0
   12 CONTINUE
      VOL = (3.1416*(3.5*2.54)**2 )/(4.0*10.0)
      CONC = GRAM/VOL
      DEPTH = GRAM*0.0261
      POR = CONC/1040.
      DO 40 I = 1,9
   40 M(I) = I
      N = NUM
      WRITE(6,61) NRUN, CONC
      WRITE(6,62)
      WRITE(6,63)  (M(I), I = 1,9)
      MIN(1) = 0
      DO 13 L = 1,N
   13 MIN(L + 1) = MIN(L) + 1
      DO 51 I = 1,9
      JJ = 1
      L = 2
      J = 1
   52 IF( TIME(I,J).GT.MIN(L) ) GO TO 50
   59 J = J + 1
      IF( J.GE.N ) GO TO 51
      GO TO 52
   50 DATAI(I,JJ) =DATA(I,J-1)+ ( DATA(I,J-1) - DATA(I,J) )/(TIME(I,J-1)
     1 - TIME(I,J) )*( MIN(L) - TIME(I,J) )
      JJ = JJ + 1
      L = L + 1
      GO TO 59
   51 CONTINUE
      NJJ = JJ + 1
      JJ = 1
      DO 14 L = 2,NJJ
      WRITE(6,60) MIN(L),  (DATAI(I,JJ), I = 1,9)
      JJ = JJ + 1
   14 CONTINUE
      DLIM = 0.50
   54 CONTINUE
      DO 57 I = 1,9
      J = 1
   56 IF( DATA(I,J).GE.DLIM ) GO TO 55
      J = J + 1
      IF( J.LT.N ) GO TO 56
```

```
      GO TO 53
   53 TOP(I) = 1.0E+20
      GO TO 57
   55 TOP(I) = TIME(I,J)
   57 CONTINUE
      WRITE(6,70)
      WRITE(6,65) DLIM
      WRITE(6,75) NRUN, CONC
      DO 58 I = 1,9
      NDIST(I) = I*10
   58 WRITE(6,66) NDIST(I), TOP(I)
      SUMY = 0.0
      SUMX = 0.0
      SUMXX = 0.0
      SUMYY = 0.0
      COUNT = 1.0
      DO 16 I = 1,9
      IF( TOP(I).GT.1000. ) GO TO 16
      COUNT = COUNT + 1.0
      SUMX = SUMX + NDIST(I)
      SUMY = SUMY + TOP(I)
      SUMXX = SUMXX + NDIST(I)**2
      SUMYY = SUMYY + TOP(I)**2
   16 CONTINUE
      YMEAN = SUMY/( COUNT - 1.0)
      XMEAN = SUMX/( COUNT - 1.0)
      XX = SUMXX - XMEAN*SUMX
      YY = SUMYY - YMEAN*SUMY
      NDF = ABS( COUNT - 3.0 )
      SUMSQ = 0.0
      SUMXY = 0.0
      DO 15 I = 1,9
      IF( TOP(I).GT.1000. ) GO TO 15
      DIFFY = TOP(I) - YMEAN
      DIFFX = NDIST(I) - XMEAN
      SUMSQ = SUMSQ + (DIFFX**2)
      SUMXY = SUMXY + (DIFFX*DIFFY)
   15 CONTINUE
      SLOPE = SUMXY/SUMSQ
      XAXIS = ( 100. - XMEAN )*SLOPE + YMEAN
      VEL = 1.0/SLOPE
      YAXIS = XMEAN - YMEAN/SLOPE
      FLUX = CONC*VEL*0.001
      BVEL = VEL/( 1.0 - POR )
      BFLUX = CONC*BVEL*0.001
      R = SLOPE*SQRT( XX/YY )
      WRITE(6,67)  VEL
      WRITE(6,74)  FLUX
      WRITE(6,80)  BVEL
      WRITE(6,81)  BFLUX
      WRITE(6,78)  DEPTH
      WRITE(6,79)  POR
      WRITE(6,68) YAXIS
      WRITE(6,69) XAXIS
      WRITE(6,76)  R
      WRITE(6,77)  NDF
      WRITE(6,71)
      WRITE(6,72) (M(I), I = 1,9)
      WRITE(6,73)  (DATA(I,1), I = 1,9)
      GO TO 17
   99 STOP
   20 FORMAT( A5 )
   21 FORMAT( 5X, 9F6.2 )
   23 FORMAT( 2F10.4 )
   60 FORMAT( 1X, I9, 20X, 9( 2X, F6.3, 2X ) )
   61 FORMAT( 1H1, 10X, 16HBATCH RUN NUMBER, A5, 10X, 13HCONCENTRATION,
     1F13.2, 2X, 10H( GM/LIT ) ////)
   62 FORMAT( 5X, 12HTIME ( MIN ), 43X, 14HCHANNEL NUMBER  /)
   63 FORMAT( 3 X, 9( 2X, I5, 2X )/)
   64 FORMAT( 5X, 11F10.3 )
   65 FORMAT( 25X, 58HTIME FOR TRANSMITTED LIGHT AT EACH POSITION TO INC
     1REASE TO , F5.2 ///)
```

```
   66 FORMAT( 30X, 23HDISTANCE FROM SURFACE  , I4, 7H ( CM ), 10X, 6HTIM
     1E  , F6.2, 8H ( MIN )/)
   67 FORMAT( 25X, 37HLINEARIZED RATE OF FALL OF INTERFACE , F8.2, 11H (
     1 CM/MIN ), //)
   68 FORMAT( 30X, 24HINTERCEPT ON DEPTH AXIS ,F8.2, 7H ( CM ), /)
   69 FORMAT( 30X, 24HINTERCEPT ON TIME AXIS  ,F8.2, 8H ( MIN )/)
   70 FORMAT( 1H1 )
   71 FORMAT( 25X, 57HINITIAL READING FOR EACH POSITION AT TIME EQUAL TO
     1 ZERO       //)
   72 FORMAT( 10X, 15HCHANNEL NUMBER , 9I10 /)
   73 FORMAT( 10X, 15HINITIAL READING, 9F10.3 )
   74 FORMAT( 30X, 19HBATCH FLUX, F10.4, 18H ( GM/SQ.CM.*MIN ) /)
   75 FORMAT(       10X, 16HBATCH RUN NUMBER, A5, 10X, 13HCONCENTRATION,
     1F13.2, 2X, 10H( GM/LIT ) ////)
   76 FORMAT( 30X, 28HCORRELATION COEFFICIENT R = , F5.3 / )
   77 FORMAT( 30X, 28HNUMBER OF DEGREES OF FREEDOM, I5, ///)
   78 FORMAT( 30X, 19HFINAL SETTLED DEPTH, F8.3,  7H ( CM ) /)
   79 FORMAT( 30X, 25HVOLUME FRACTION OF SOLIDS, F6.3 / )
   80 FORMAT( 30X, 34HVELOCITY CORRECTED FOR RETURN FLOW, F8.2, 11H ( CM
     1/MIN ) /)
   81 FORMAT( 30X, 36HBATCH FLUX CORRECTED FOR RETURN FLOW, F10.4, 18H (
     1 GM/SQ.CM.*MIN ) /)
      END
C        6400 END OF RECORD
C     NRUN = ALPHANUMERIC WORD IDENTIFYING RUN
C     SCAN = TIME REQUIRED FOR SCANNER TO SCAN 100 CHANNELS
C     GRAM = CUMULATIVE WEIGHT, IN GRAMS, OF PARTICLES IN COLUMN
C           END OF FILE
```

PROGRAM NUMBER 3

```
      CONTINUOUS SETTLER DATA REDUCTION
      PROGRAM TST (INPUT,OUTPUT,TAPE5=INPUT,TAPE6=OUTPUT)
      DIMENSION VOLT(10,90), QU(90), QO(90), QF(90), GU(90), GF(90), KLE
     1R(90), FCONC(90), UCONC(90),ABSN(10,90), FABSN(10,90), TIME(90)
      READ(5,20)  N
      WRITE(6,20)  N
      DO 10 J = 1,N
   10 READ(5,21) (VOLT(I,J),I = 1,9), QU(J), QO(J),QF(J), GU(J), GF(J),
     1TIME(J),KLER(J)
      WRITE(6,30)((VOLT(I,J),I = 1,9),QU(J), QO(J), QF(J), GU(J), GF(J),
     1 TIME(J), KLER(J),J = 1,N )
      DO 12 J = 1,N
      K = KLER(J)
      IF( GF(J) ) 14,14,15
   15 FCONC(J) = GF(J)/QF(J)*1000.0
      UCONC(J) = GU(J)/QU(J)*1000.0
   14 DO 11 I= 1,9
      ABSN(I,J) = VOLT(I,K) - VOLT(I,J)
      FABSN(I,J) = VOLT(I,J) / VOLT(I,K)
   11 CONTINUE
      WRITE(6,22)  J,TIME(J)
      IF( GF(J) ) 16,16,17
   17 WRITE(6,23)
      WRITE(6,24) QF(J), GF(J), FCONC(J)
      WRITE(6,29) QU(J), GU(J), UCONC(J)
      WRITE(6,25) QO(J)
      FLUX = ((GU(J) + GF(J))/2.0)/((3.1416*(3.5*2.54)**2)/4.0)
      WRITE(6,31) FLUX
      GO TO 18
   16 WRITE(6,28)
   18 WRITE(6,26)
      DO 13 I = 1,9
   13 WRITE(6,27) I, ABSN(I,J), FABSN(I,J)
   12 CONTINUE
      STOP
   20 FORMAT( I5 )
   21 FORMAT( 9F5.2, 3F4.0, 2F8.4, F5.1, I2 )
   22 FORMAT( 1H1, 30X, 13HRUN NUMBER = , I5, 10X, 10HAT TIME = , F5.1,
     1 6H HRS.  /// )
   23 FORMAT( 25X, 20HFLOW RATE ( ML/MIN ), 10X, 22HSOLIDS FLUX ( GM/MIN
     1 ), 10X,  24HCONCENTRATION ( GM/LIT )  / )
   24 FORMAT( 18X, 13H     FEED     , F4.0, 22X, F8.4, 26X, F6.2 / )
   25 FORMAT( 18X, 13H OVERFLOW    ,F4.0 / // )
   26 FORMAT( 20X, 61HLIGHT READING CORRECTED FOR ZERO CONCENTRATION AND
     1 NORMALIZED  ///)
   27 FORMAT( 40X, 11HCHANNEL NO., I4, 10X,F5.2, 10X, F6.4 / )
   28 FORMAT( 31X, 25HCONCENTRATION EQUALS ZERO //)
   29 FORMAT( 18X, 13HUNDERFLOW     , F4.0, 22X, F8.4, 26X, F6.2 / )
   30 FORMAT( 10X, 9F7.2, 3F7.0, 2F11.4, F8.1, I6 )
   31 FORMAT( 30X, 26HAVERAGE FLUX PER UNIT AREA, F10.3, 19H  ( GM/SQ.CM
     1.*MIN ) ///)
      END
        6400 END OF RECORD
      N = NUMBER OF DATA SETS
        6400 END OF FILE
```

APPENDIX D

Additional References

1. Alger, G.R. and Simon, D.B.
   Fall Velocity of Irregular Shaped Particles
   ASCE, J. Hyd. Div., 94, HY3, 721 (1968)

2. Anderson, A.A. and Sparkman, J.E.
   Review Sedimentation Theory
   Chem. Eng., Nov. 2, 75 (1959)

3. Anderson, N.E.
   Design of Final Settling Tanks for Activated Sludge
   Sew. Wks J., 17, 50 (1945)

4. Behn, V.C.
   Settling Behaviour of Waste Suspensions
   ASCE, J. San. Eng. Div., 83, SA5, 1 (1957)

5. _____ ; and Liebman, J.C.
   Analysis of Thickener Operation
   ASCE, J. San. Eng. Div., 89, SA3, 1 (1963)

6. Betz, J.M.
   The Valley Settling Basin Facilities, Los Angeles, Calif.
   Sew. & Ind. Was., 29, 667 (1957)

7. Bloodgood, D.E.; Boegly, W.U. and Smith, C.E.
   Sedimentation Studies
   ASCE, 82, SA5, 1083 (1956)

8. _____ ; _____ ; and _____ ;
   Sedimentation Studies,
   ASCE, J. San. Eng. Div., 82, SA5, 1083 (1956)

9. Bond, A.W.
   Behaviour of Suspensions
   ASCE, J. San. Eng. Div., 86, SA3, 57 (1960)

10. _____ ;
    The Behaviour of Suspensions
    J. Instn. Wat. Engrs., 15, 474 (1961)

11. _____ ;
    Upflow Solids Contact Basin
    ASCE, J. San. Eng. Div., 87, SA3, 73 (1961)

12. Bramer, H.C. and Hoak, R.D.
    Design Criteria for Sedimentation Basins
    I & EC (Proc. Des. Div.), 1, 185 (1962)

13. Bramer, H.C. and Hoak, R.D.
Some Observations on Liquid Solids Separations with Particle Growth
20th Indust. Was. Conf., Purdue (1965), p.423

14. Camp, T.R.
A Study of the Rational Design of Settling Tanks
Sew. Wks. J., 8, 742 (1936)

15. _____ ;
Sedimentation and the Design of Settling Tanks
Trans. ASCE 111, 895 (1946)

16. _____ ;
Studies of Sedimentation Basin Design
Sew. & Ind. Was., 25, 1, 1 (1953)

17. Carpenter, L.V. and Speider, H.
Notes on Sedimentation
Sew. Wks. J., 7, 200 (1935)

18. Chodak, M.E.
Operation of Continuous Thickeners
Eff. & Wat. Treat. J., 2, 445 (1962)

19. Clifford, W. and Windridge, M.E.D.
The Settlement of Activated Sludge
Proc. Inst. Sew. Purification, 115 (1932)

20. Conway, R.A. and Edwards, V.A.
How to Design Sedimentation Systems from Laboratory Data
Chem. Eng., 68, 19, 167 (1961)

21. Culp, G.L.; Hsiung, K.Y.; and Conley, W.R.
Tube Clarification Process, Operating Experiences
ASCE, J. San. Eng. Div., 95, SA5, 829 (1969)

22. Daniels, S.L.
The Utility of Optical Parameters in Evaluation of Processes of Flocculation and Sedimentation
AIChE, Chem. Eng. Progress Symp. Series 97 (Water - 1969), 95, (1968) p.171

23. Dick, R.I. and Ewing, B.B.
Evaluation of Activated Sludge Thickening Theories
ASCE, J. San. Eng. Div., 93, SA4, 9 (1967)

24. Dick, R.I.
Applicability of Prevailing Gravity Thickening Theories to Activated Sludge
Ph.D Thesis, U. of Ill., Urbana (1969)

25. Dick, R.I.
Sedimentation
Wat. & Was. Eng., 6, 2, 47 (1969)

26. _____ ;
Fundamental Aspects of Sedimentation
Wat. & Was. Eng., 6, 3, 47 (1969)

27. _____ ;
Role of Activated Sludge Settling Tanks
ASCE, J. San. Eng. Div., 96, SA2, 423 (1970)

28. Eckenfelder, W.W. and Melbinger, N.
Settling and Compaction Characteristics of Biological Sludges
J. WPCF, 29, 10, 1114 (1957)

29. Edde, H.J. and Eckenfelder, W.W.
Theoretical Concepts of Gravity Sludge Thickening
J. WPCF, 40, 8, 1486 (1968)

30. Egolf, C.B. and McCabe, W.L.
Rate of Sedimentation of Flocculated Particles
Trans. AIChE, 33, 620 (1932)

31. Fielder, R.A. and Fitch, E.B.
Appraising Basin Performance from Dye Test Studies
Sew. & Ind. Was., 31, 1016 (1959)

32. Fitch, E.B.
Why Particles Separate in Sedimentation Process
I & EC, 54, 10, 44 (1962)

33. _____ ;
Current Theory and Thickener Design
I & EC, 58, 10, 18 (1966)

34. _____ ;
A Mechanism of Sedimentation
I & EC (Fundamentals), 5, 1, 139 (1966)

35. Gaudin, A.M. and Fuerstenau, M.C.
Experimental and Mathematical Model of Thickening
Soc. Min. Engrs., 233, 122 (1962)

36. Hansen, S.R. and Culp, G.L.
Applying Shallow Depth Sedimentation Theory
J. AWWA, 59, 9, 1134 (1967)

37. Hazen, A.
On Sedimentation
Trans. ASCE, 53, 45 (1904)

38. Ingersoll, A.C.; McKee, I.E. and Brook, N.H.
Fundamental Concepts of Rectangular Settling Tanks
Trans. ASCE, 121, 1179 (1956)

39. Jordan, V.J. and Scherer, C.H.
Gravity Thickening Techniques at a Water Reclamation Plant
J. WPCF, 42, 1, 180 (1970)

40. Kalinske, A.A.
Settling Characteristics of Suspensions in Water Treatment Processes
J. AWWA, 40, 113 (1948)

41. _____ ;
Settling Rate of Suspensions in Solids Contact Units
Proc. ASCE, 76, 186 (1953)

42. Katz, W.J.; Geinopolos, A. and Mancini, J.L.
Concepts of Sedimentation Applied to Design
Wat. & Sew. Wks., 109, 162 (1962)

43. Keeferer, C.E.
Thickening of Raw Sludges
Wat. & Sew. Wks., 107, 6, 218 (1960)

44. Lee, C.A.
Sedimentation and Design of Sedimentation Pits
Wat. & Sew. Wks., 117, 3, 93 (1970)

45. Mancini, J.L.
Gravity Clarifier and Thickener Design
17th Indust. Wat. Conf., Purdue (1962) p.267

46. _____ and Eckenfelder, W.W.
Thickening of Industrial Sludges
5th Ind. Wat. & Was. Conf., Texas (1965) p.64

47. McGauhey, P.H.
Theory of Sedimentation
J. AWWA, 48, 437 (1956)

48. Michaels, A.S. and Bolger, J.C.
Settling Rates and Sediment Volumes of Flocculated Kaolin Suspensions
I & EC (Fundamentals), 1, 24 (1962)

49. Miller, D.G.
Sedimentation - A Review of Published Work
Wat. & Was. Eng., 68, 2, 52 (1964)

50. Mueller, H.M.
High Rate Sedimentation and Filtration
Wat. & Was. Eng., 7, 6, 65 (1970)

51. Poepel, F.
Settling Tank Design
Wat. & Sew. Wks., 97, 422 (1950)

52. Prager, F.D.
The Sludge Blanket Clarifier
Wat. & Sew. Wks., 97, 143 (1950)

53. Ratcliff, G.A.; Blackadder, D.A. and Sutherland, A.N.
Compressibility of Sediments
Chem. Eng. Sci., 22, 2, 201 (1967)

54. Robinson, C.S.
Some Factors Affecting Sedimentation
I & EC, 18, 869 (1926)

55. Rudolfs, W. and Lacy, I.O.
Settling and Compacting of Activated Sludge
Sew. Wks. J., 6, 4, 647 (1934)

56. Schwepfer, G.J.
Factors Affecting the Efficiency of Sewage Sedimentation
Sew. Wks. J., 5, 209 (1933)

57. Shannon, P.T.; Schaas, R.D.; Stroupe, E.P. and Tory, E.M.
Batch and Continuous Thickening
I & EC (Fundamentals), 3, 4, 250 (1964)

58. Sparr, A.E. and Grippi, V.
Gravity Thickeners for Activated Sludge
J. WPCF, 41, 11, 1886 (1969)

59. Tesarik, I.
Flow in Sludge Blanket Clarifiers
ASCE, J. San. Eng. Div., 93, SA6, 105 (1967)

60. Tory, E.M. and Shannon, P.T.
Reappraisal of the Concept of Settling in Compression
I & EC (Fundamentals), 4, 194 (1965)

61. Vesiland, P.A.
Influence of Stirring on Thickening of Biological Sludge
Ph.D Thesis, U. of N. Carolina (1968)

62. _____ ;
Design of Protype Thickeners from Batch Settling Tests
Wat. & Sew. Wks., 115, 7, 202 (1968)

63. Vesiland, P.A.
Design of Thickness from Batch Settling Tests
Wat. & Sew. Wks., 115, 9, 418 (1968)

64. Work, L.T. and Kohler, A.S.
Sedimentation of Suspensions
I & EC, 32, 1329 (1940)

65. Yao, K.M.
Theoretical Study of High-Rate Sedimentation
J. WPCF, 42, 1, 218 (1970)

66. Yoshioka, N.; Hotta, Y. and Tanaka, S.
Batch Settling of Homogeneous Slurries
Kaguku Kogaku, 19, 616 (1955) (Chem. Eng. Japan)

67. _____ ; _____ ; _____ ; Naito, S.; Tsugami, S.
Continuous Thickening of Homogenous Flocculated Slurries
IBID, 21, 66 (1957)

68. Zuber, N.
On the Dispersed Two-Phase Flow in the Laminar Flow Regime
Chem. Eng. Sci., 19, 897 (1964)